Probabilities of Large Earthquakes in the San Francisco Bay Region, California

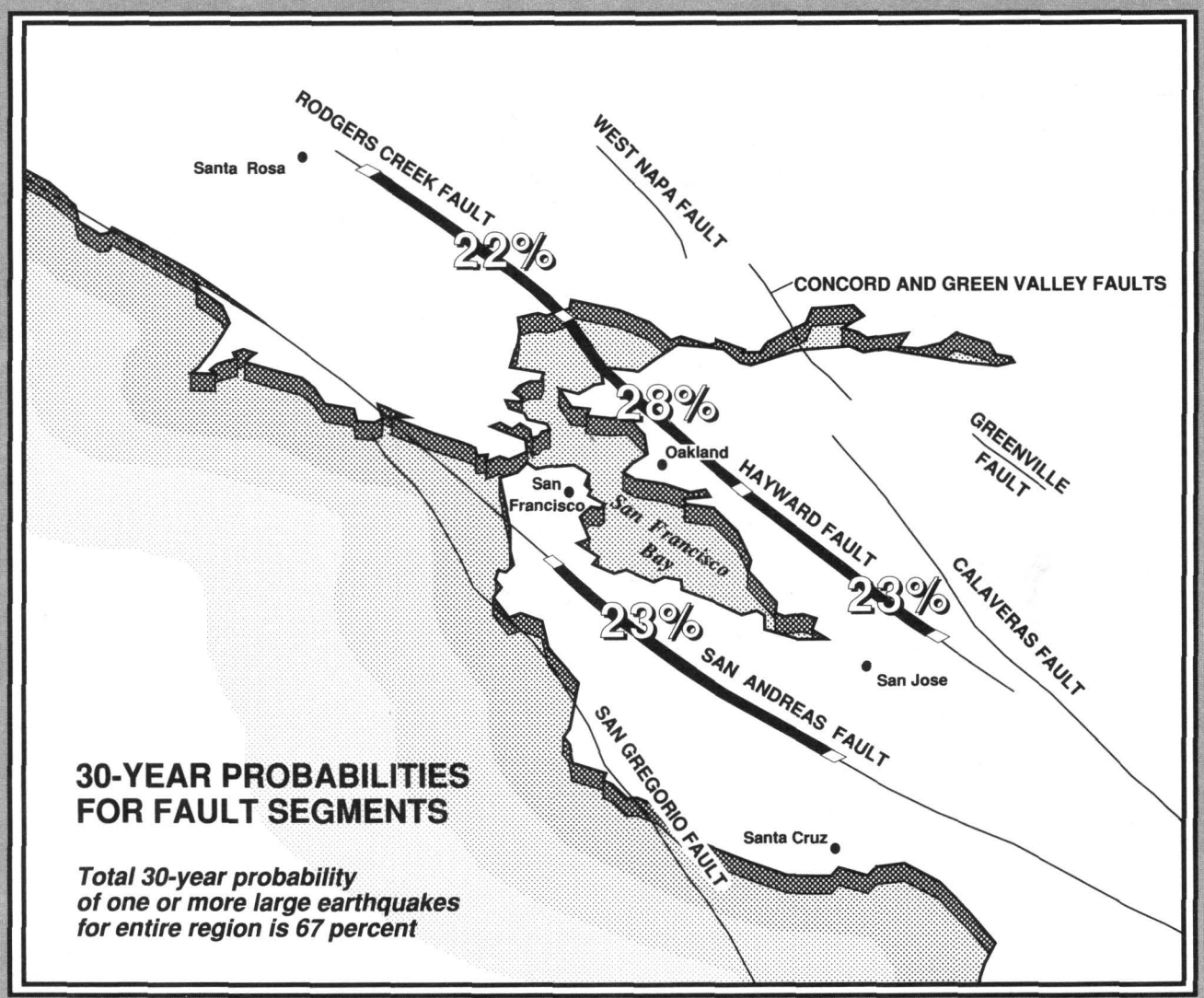

U.S. GEOLOGICAL SURVEY CIRCULAR 1053

Probabilities of Large Earthquakes in the San Francisco Bay Region, California

By WORKING GROUP ON CALIFORNIA EARTHQUAKE PROBABILITIES

U.S. GEOLOGICAL SURVEY CIRCULAR 1053

DEPARTMENT OF THE INTERIOR
MANUEL LUJAN, JR., Secretary

U.S. GEOLOGICAL SURVEY
Dallas L. Peck, Director

UNITED STATES GOVERNMENT PRINTING OFFICE, WASHINGTON : 1990

Free on application to the
Books and Open-File Reports Section
U.S. Geological Survey
Federal Center, Box 25425
Denver, CO 80225

WORKING GROUP ON CALIFORNIA EARTHQUAKE PROBABILITIES

James H. Dieterich, Chairman	U.S. Geological Survey
Clarence R. Allen	California Institute of Technology
Lloyd S. Cluff	Pacific Gas & Electric Co.
C. Allin Cornell	Stanford University
William L. Ellsworth	U.S. Geological Survey
Lane R. Johnson	University of California, Berkeley
Allan G. Lindh	U.S. Geological Survey
Stuart P. Nishenko	U.S. Geological Survey
Chris H. Scholz	Lamont-Doherty Geological Observatory, Columbia University
David P. Schwartz	U.S. Geological Survey
Wayne Thatcher	U.S. Geological Survey
Patrick L. Williams	Lawrence Berkeley Laboratory

PREFACE

In 1987 a Working Group on California Earthquake Probabilities was organized by the U.S. Geological Survey at the recommendation of the National Earthquake Prediction Evaluation Council (NEPEC). The membership included representatives from private industry, academia, and the U.S. Geological Survey. The Working Group computed long-term probabilities of earthquakes along the major faults of the San Andreas fault system on the basis of consensus interpretations of information then available. Faults considered by the Working Group included the San Andreas fault proper, the San Jacinto and Imperial faults of southern California, and the Hayward fault of northern California. The Working Group issued a final report of its findings in 1988 (Working Group, 1988) that was reviewed and endorsed by NEPEC.

As a consequence of the magnitude 7.1 Loma Prieta, California, earthquake of October 17, 1989, a second Working Group on California Earthquake Probabilities was organized under the auspices of NEPEC. Its charge was to review and, as necessary, revise the findings of the 1988 report on the probability of large earthquakes in the San Francisco Bay region. In particular, the Working Group was requested to examine the probabilities of large earthquakes in the context of new interpretations or physical changes resulting from the Loma Prieta earthquake. In addition, it was to consider new information pertaining to the San Andreas and other faults in the region obtained subsequent to the release of the 1988 report. Insofar as modified techniques and improved data have been used in this study, the same approach might also, of course, modify the probabilities for southern California. This reevaluation has, however, been specifically limited to the San Francisco Bay region.

This report is intended to summarize the collective knowledge and judgments of a diverse group of earthquake scientists to assist in formulation of rational earthquake policies. A considerable body of information about active faults in the San Francisco Bay region leads to the conclusion that major earthquakes are likely within the next tens of years. Several techniques can be used to compute probabilities of future earthquakes, although there are uncertainties about the validity of specific assumptions or models that must be made when applying these techniques. The body of this report describes the data and detailed assumptions that lead to specific probabilities for different fault segments. Additional data and future advances in our understanding of earthquake physics may alter the way that these probabilities are estimated. Even though this uncertainty must be acknowledged, we emphasize that the findings of this report are supported by other lines of argument and are consistent with our best understanding of the likelihood for the occurrence of earthquakes in the San Francisco Bay region.

CONTENTS

FIGURES

TABLES

Probabilities of Large Earthquakes in the San Francisco Bay Region, California

By Working Group on California Earthquake Probabilities

EXECUTIVE SUMMARY

In 1988 a Working Group convened by the National Earthquake Prediction Evaluation Council (NEPEC) issued a report (Working Group, 1988) assessing the long-term probabilities of large earthquakes (magnitude 7 or greater) along the San Andreas fault system. NEPEC organized the present Working Group to reexamine the probabilities of large earthquakes in the San Francisco Bay region, in light of new interpretations or physical changes resulting from the Loma Prieta earthquake of October 17, 1989, and new data developed since the 1988 report.

We now estimate the chance of one or more large earthquakes in the San Francisco Bay region in the coming 30 years to be about 67 percent. A magnitude 7 or larger earthquake along any of the segments considered by the Working Group will have a major impact on the entire San Francisco Bay region.

The first step in the evaluation procedure is to identify fault segments expected to produce large earthquakes, and then to estimate the time to the next earthquake on each identified segment. The recurrence times for earthquakes on a segment are based on the records of historic earthquakes, the long-term slip rate, and the displacement in the previous earthquake. The approach followed for calculation of probabilities employs the estimated recurrence times with a model that assumes that probability increases with elapsed time from the last large earthquake on a fault segment. The minimum information required for this analysis of the San Francisco Bay region is available only for the San Andreas, Hayward, and Rodgers Creek faults. Other potentially important faults in the region will require more study before they can be evaluated. Hence, the calculated probabilities are necessarily a minimum estimate of the hazard.

Principal changes from the 1988 report and new factors considered by the Working Group that affect the estimates of probabilities are

- Addition of the Rodgers Creek fault segment. Data on the Rodgers Creek fault (see map of 30-year probabilities on following page) collected since 1988 permit probabilistic assessment of that fault for the first time.
- Faster fault-slip rates. Estimates of the long-term rates of slip on the San Andreas and Hayward faults are revised upward relative to the previous estimates. A higher slip rate shortens the expected time to the next earthquake and increases the likelihood of an earthquake. The Working Group estimates the slip rate on the San Andreas fault within the San Francisco Bay region to be 19 mm/yr compared to the previous (1988) Working Group estimate of 16 mm/yr. The slip rate on the Hayward fault is now estimated at 9 mm/yr compared to the previous estimate of 7.5 mm/yr.

Manuscript approved for publication, July 19, 1990.

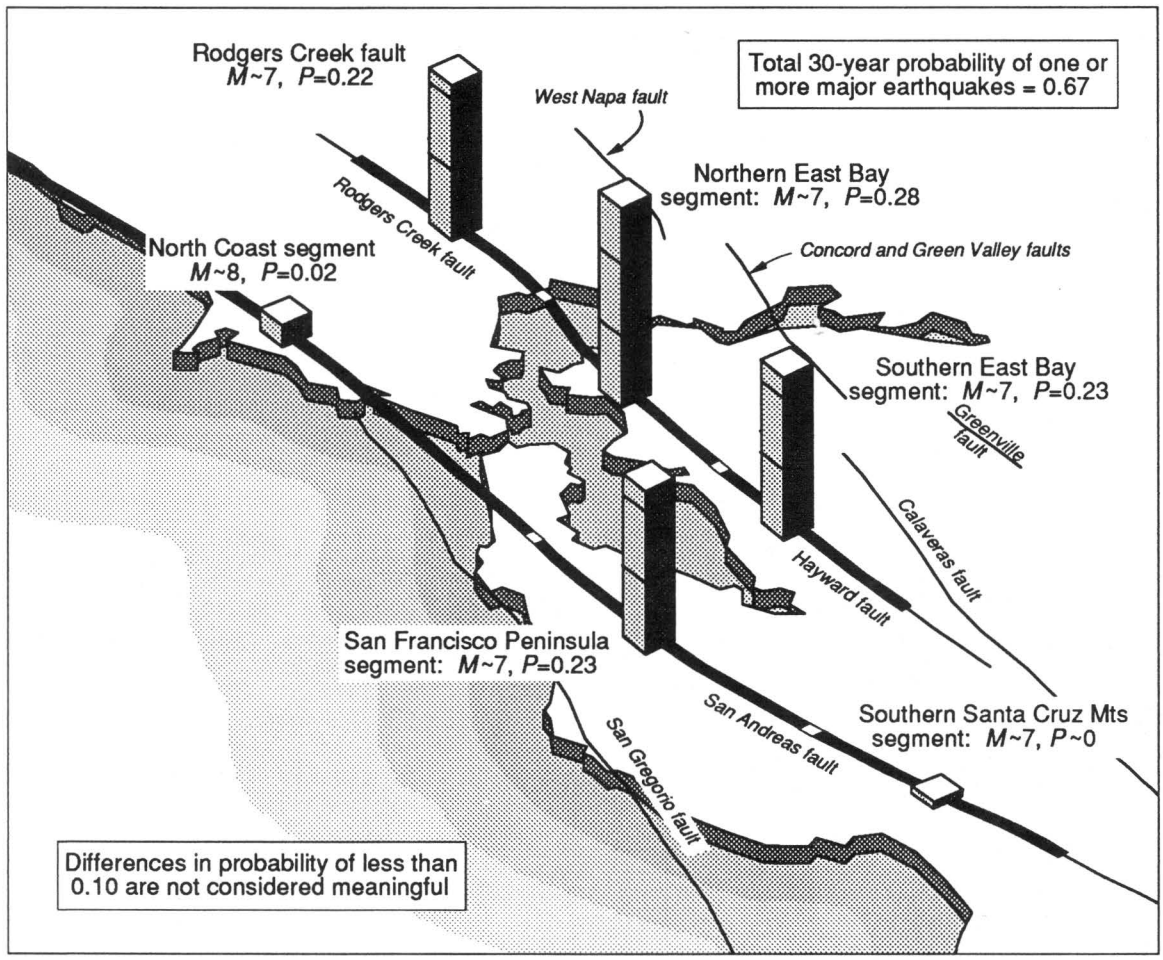

30-YEAR PROBABILITIES (*P*) OF LARGE EARTHQUAKES (*M*≥7) IN THE SAN FRANCISCO BAY REGION

Column heights are proportional to 30-year probability of earthquake rupture

- Effects of the Loma Prieta earthquake on the San Andreas fault. The probability of an earthquake on the segment where the Loma Prieta earthquake occurred (southern Santa Cruz Mountains segment) is low following that earthquake. Models of crustal deformation indicate that stress increased on nearby segments of the San Andreas fault as a result of the Loma Prieta earthquake. The stress increase shortens the time to the next earthquake on these segments. However, it is not known if the magnitude of this effect is large enough to be significant.

Because the quality of the data, the uncertainties relating to segmentation, and the uncertainties in application of the model vary from segment to segment, the Working Group has assigned letter grades to indicate its judgment of the reliability of the calculated probabilities. The reliability scale extends from A to E with A being the most reliable. Probabilities are expressed as numbers that range between 0 and 1. Differences of probability of less than 0.10 are not considered meaningful. A 30–year probability of 0.20 means there is a 20–percent chance of an earthquake in the coming 30 years. The probabilities for the seven segments considered in this report are summarized in the following table.

Probabilities of earthquakes on fault segments in the San Francisco Bay region

Segment	Previous event	Expected magnitude	Probability 1990–2020	Level of reliability (scaled A to E; A most reliable)
San Andreas fault				
S. Santa Cruz Mountains	1989	7	<0.01	B
San Francisco Peninsula	1906	7	.23	C
North Coast	1906	8	.02	B
Hayward fault				
Southern East Bay	1868	7	.23	C
Northern East Bay	1836	7	.28	D
Rodgers Creek fault	1808 (or earlier)	7	.22	D

- Four fault segments have been identified that have a probability in the range 0.20 to 0.30 of producing a large earthquake (magnitude about 7) in the coming 30 years.
- The probability of a magnitude 7 earthquake along the southern Santa Cruz Mountains segment that produced the 1989 Loma Prieta earthquake is now less than 0.01. The previous study (Working Group, 1988) had assigned a probability of 0.3 to this segment prior to the earthquake.

Although the potential for damage from an earthquake generally decreases as distance from the epicentral region increases, the pattern of losses at rather large distances from the magnitude 7.1 Loma Prieta earthquake clearly demonstrates that an earthquake on any of the fault segments considered by the Working Group could seriously affect the entire San Francisco Bay region. Indeed, the most densely populated parts of the area lie atop of, or adjacent to, fault segments having the greatest potential for large earthquakes.

The probability that the San Francisco Bay region will experience at least one large earthquake on the segments considered is given by the following table.

Probabilities of one or more large earthquakes in the San Francisco Bay region

Segments	Probability for intervals beginning 1/1/90				Level of reliability (A to E; A most reliable)
	5 yr	10 yr	20 yr	30 yr	
North Coast, San Francisco Peninsula, N. East Bay, S. East Bay, and Rodgers Creek	0.15	0.33	0.50	0.67	B

The probability of one or more large earthquakes in the San Francisco Bay region in the coming 30 years is now estimated to be 0.67. The previous NEPEC Working Group (Working Group, 1988) found the probability to be about 0.5, but that aggregate probability did not include either the southern Santa Cruz Mountains segment or the Rodgers Creek fault. About half of the increase of probability from the previous report can be ascribed to adding the Rodgers Creek fault segment to the list of major earthquake sources. The remaining increase is due to smaller increases of the probabilities of earthquakes on the previously recognized fault segments, resulting primarily from new estimates of fault–slip rate. We consider these aggregate probabilities to be significantly more reliable than the probabilities of earthquakes on individual segments.

These cumulative probabilities for large earthquakes in the San Francisco Bay region are consistent with the observed rate of occurrence of such events during the 19th century. The average (Poisson) 30–year probability of earthquakes greater than magnitude 7 since 1836 is 0.5, and the somewhat higher value of about 0.7 estimated here reflects the higher rate of activity that is expected as the post–1906 earthquake quiescence ends and the 19th–century activity level resumes.

This study was limited to evaluating the probabilities of large earthquakes on the San Andreas, Hayward, and Rodgers Creek faults. In the present assessment, these faults account for only 28 mm/yr of the 33 to 40 mm/yr of deformation that takes place across the entire San Andreas fault system in the region. Some or all of this unaccounted–for deformation may represent a potential for earthquakes on other important faults in the San Francisco Bay region, such as the Calaveras, Concord, Greenville, Green Valley, and San Gregorio faults. At present, however, there is not sufficient information to specifically address the time–dependent probability of earthquakes originating along these other faults. Hence, the probabilities reported here should be regarded as minimum values.

The assessment of long–term seismic hazard on California's major faults continues to be a rapidly developing field. Models for the determination of probabilities and the data employed in those models are subject to uncertainty and alternate interpretations. In the future, new data and more refined models will undoubtedly lead to somewhat different probabilities for specific fault segments. However, the total aggregated probabilities are less sensitive to the detailed recurrence characteristics of the individual segments. This characteristic of the aggregated probabilities supports the principal conclusion of this study: **There is a high likelihood of a major earthquake in the San Francisco Bay region within the next 30 years.**

INTRODUCTION

The October 17, 1989, Loma Prieta earthquake caused 62 deaths, 3,757 injuries, and more than $6 billion in property damage (Plafker and Galloway, 1989). Earthquakes of comparable or larger size will certainly occur along other, more densely populated segments of the San Andreas and Hayward faults. Such earthquakes will result in far greater losses than experienced from the 1989 earthquake. For example, about 1,260,000 people live within the epicentral region[1] of an expected magnitude 7 earthquake along the northern East Bay segment of the Hayward fault. That is about 10 times as many people as the 130,000 who live within the epicentral region of the Loma Prieta earthquake (Brian Kilgore, written commun., 1989).

The record of past earthquakes, along with related geodetic, geologic, and seismic observations, provides the principal means for evaluating the potential for future earthquakes. With the occurrence of the 1989 Loma Prieta earthquake, California has now experienced at least 12 large earthquakes of magnitude 7 or greater since 1812. Five of these earthquakes affected the greater San Francisco Bay region. The San Andreas fault on the San Francisco Peninsula produced the earthquake of 1838 (probable magnitude 7) and the great earthquake of 1906 (magnitude about 8). Additionally there was the earthquake of 1865 that appears similar to the recent Loma Prieta earthquake and possibly affected the same segment of the San Andreas fault south of the San Francisco Peninsula. Along the eastern side of San Francisco Bay, earthquakes of about magnitude 7 originated on the Hayward fault in 1836 and 1868.

The 1988 Working Group estimated the 30–year probability of one or more magnitude 7 earthquakes in the San Francisco Bay region to be 0.5. This probability was aggregated from the probabilities computed for individual fault segments, which included the San Francisco Peninsula segment of the San Andreas fault and two segments of the Hayward fault (the northern East Bay segment and the southern East Bay segment). An additional segment, the southern Santa Cruz

[1] The epicentral region is the area of most intense ground motion on bedrock sites and is, for this example, defined as the area lying within 10 km of the earthquake fault rupture.

Mountains segment at the southern end of the San Francisco Peninsula segment, was not included in this aggregation, because the reliability of the forecast was considered to be low and because the earthquake was expected to have a magnitude less than 7. However, this segment had a higher 30–year probability (0.3) than any other segment in the region. Within the uncertainty associated with the definition of fault segments, the October 17, 1989, magnitude 7.1 Loma Prieta earthquake occurred on the southern Santa Cruz Mountains segment.

The principal reason for undertaking this review of San Francisco Bay region probabilities was the occurrence of the Loma Prieta earthquake. The Loma Prieta earthquake could affect probabilistic assessments in two ways. First, the earthquake provides an added source of data that may alter interpretations of earlier observations that served as the basis for probability calculations. Second, slip on the Loma Prieta earthquake segment altered the stress state on other fault segments; as a consequence of the Loma Prieta earthquake, segments may now be closer or farther from failure than they were before the earthquake.

Two additional factors provided impetus for this review. The first is new information on slip rate and earthquake recurrence for the Hayward and Rodgers Creek faults. The second is consideration of several features of the regional seismicity that may indicate an increased potential for large earthquakes. These include an apparent return to the higher rates of earthquake activity of the 1800's following a post–1906 lull in earthquake rates, migration of moderate earthquakes northward along the Calaveras fault to the southern end of the Hayward fault, and possible pairing of large earthquakes on the San Andreas fault with large earthquakes on the Hayward fault.

Methods and models for estimation of earthquake probabilities are at an early stage of development, and we expect future research to provide more refined approaches. Input parameters for the calculation of probabilities are by their nature subject to alternative interpretations that may affect specific assessments of hazard. An important emphasis of this Working Group study was to explore and weigh alternate interpretations relevant to assessing the potential for earthquakes. The development of improved methods, the acquisition of new data, and the inevitable occurrence of earthquakes in the San Francisco Bay region will necessitate future revisions of this report. However, other lines of argument, which are not dependent on the details of the probabilistic model we have employed, also lead to the conclusion that there is a significant chance of one or more large earthquakes in the region in the coming decades. Those arguments are based on historical frequency of large earthquakes and a consensus that strain energy is accumulating that will be released in future large earthquakes.

METHOD

For this report, probabilities of earthquake recurrence have been calculated following the approach described in the 1988 Working Group report. We briefly outline the method here and refer the interested reader to appendix A for additional explanation. The approach used in this study is based upon a model of earthquake occurrence that assumes that the probability of an earthquake along a fault segment is initially low following a large segment–rupturing earthquake and increases with time as stress on the segment recovers the stress drop of the prior earthquake (Rikitake, 1974; Hagiwara, 1974). Fault segments expected to rupture in coming earthquakes are delineated using a variety of observations and judgments. We have reviewed the fault segmentation employed for the 1988 report and in some cases revised segment boundaries.

Probabilities of the occurrence of the next segment–rupturing earthquake in some time interval are obtained from a probability density function for the random time of recurrence, T. We have followed the practice of the 1988 Working Group and employed the lognormal distribution. The current San Francisco Bay region forecasts are not sensitive to this particular choice of distribution function. Input parameters for the calculation of the probability of recurrence along a particular fault segment are T_e, the elapsed time since the last segment–rupturing earthquake; $\hat{T}$, the median

recurrence interval of the next segment–rupturing event; and σ, a measure of the dispersion or spread in the recurrence time distribution. Time is set to zero at the occurrence of the most recent earthquake.

The fraction of all earthquake recurrence times in an interval $(t, t + \Delta T)$ is obtained from the lognormal probability density function by integration:

$$P(t \leq T \leq t + \Delta T) = \int_t^{t+\Delta T} \frac{1}{u\sigma\sqrt{2\pi}} \exp\left\{\frac{-[\ln u/\hat{T}]^2}{2\sigma^2}\right\} du. \quad (1)$$

The probabilities we report below employ the additional knowledge that the earthquake has not occurred prior to time T_e. The probability conditional on the earthquake not having occurred prior to T_e is

$$P(T_e \leq T \leq T_e + \Delta T | T > T_e) = \frac{P(T_e \leq T \leq T_e + \Delta T)}{1 - P(0 \leq T \leq T_e)}. \quad (2)$$

Figure 1 illustrates a lognormal probability density function and the graphical interpretation of the probabilities appearing in equation (2). All probabilities reported below are conditional probabilities and employ T_e corresponding to January 1, 1990.

For every fault segment considered in this report, an estimation of the median recurrence time, $\hat{T}$, has been obtained using the time–predictable method (Reid, 1910; Shimazaki and Nakata, 1980). According to the time–predictable method, the most likely elapsed time to the next earthquake equals the slip in the last event divided by the average slip rate:

$$\hat{T} = D/V \ , \quad (3)$$

where D is the best (median) estimate of displacement in the previous segment–rupturing earthquake and V is the best (median) estimate of the long–term slip rate.

For a lognormal distribution, σ represents the standard deviation[2] of the natural logarithm of the recurrence time. We have taken as σ the total or net standard deviation, σ_N, which is the square root of the sum of the squares of two components: (1) σ_P, a parametric uncertainty in $\hat{T}$ arising from the uncertainties in D and V, and (2) σ_I, an intrinsic uncertainty which reflects the event–to–event variability in recurrence times when $\hat{T}$ is perfectly known. From the Nishenko and Buland (1987) study of the intrinsic variability of characteristic recurrence times for circum–Pacific earthquakes, an estimate of the (marginal) intrinsic uncertainty is 0.21. Because recurrence data are limited, the value of σ_I may not be well defined, particularly for strike–slip earthquakes (Savage, 1990; J.C. Savage, written commun., 1990). Uncertainty in σ_I strongly affects attempts to estimate uncertainties in the calculated probabilities (see appendix C). However, the total value of σ_N (parametric and intrinsic uncertainties combined) and consequently calculated probabilities are not very sensitive to this intrinsic value in our present application due to the larger values of the parametric uncertainty, σ_P.

Below, we review the data and interpretations that affect the determination of earthquake probabilities in the San Francisco Bay region. A method for quantitative treatment of alternate interpretations of the data for San Andreas fault segments is outlined below and presented in greater detail in appendix B.

Following the convention established by the previous Working Group report (1988), we have assigned letter grades to the consensus probabilities to indicate our judgment of the quality and completeness of the data used to estimate those probabilities. The segments are ranked from A to E. The segments judged to have the most reliable data are ranked A; E indicates the least reliable

[2] Throughout this report σ is used to indicate the standard deviation of the log of an estimate. Where it is necessary to indicate the standard deviation of an estimate, the symbol S is employed. $\pm$ values give the numerical value of the standard deviation of the estimate.

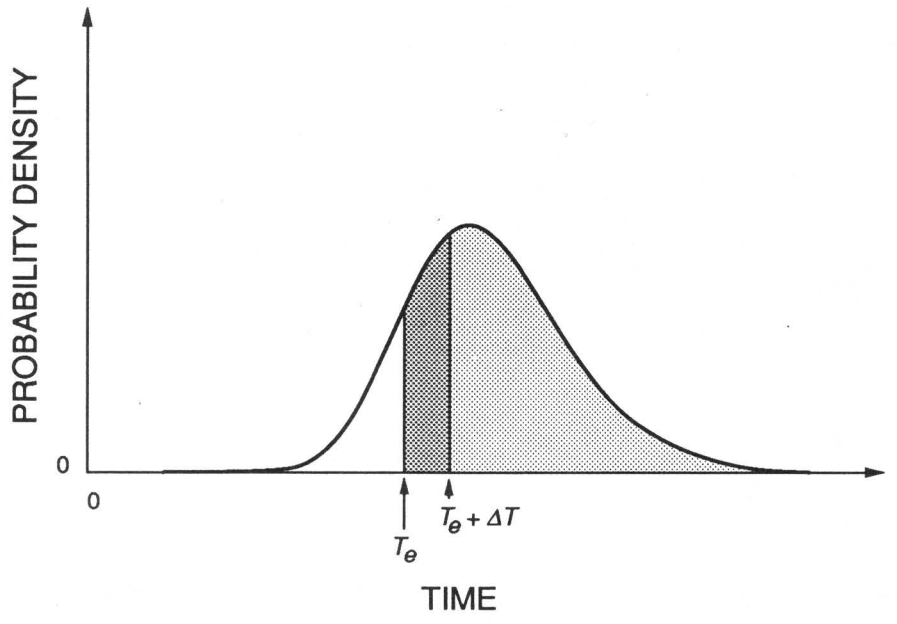

Figure 1. Probability density function for earthquake recurrence. Conditional probability in interval ($T_e \leq T \leq T_e + \Delta T$), given elapsed time T_e, is ratio of area of dark shading to sum of areas with dark and light shading.

data. For levels of reliability C, D, and E, both the evaluation of segment length (and the related magnitude) and the probability value may change significantly with additional data.

Consensus probabilities reported below are reported to two decimal places, but we emphasize that differences of less than a tenth are not considered meaningful. In appendix C we tabulate the probabilities for time intervals of 5, 10, 20, and 30 years. Appendix C includes tabulations of probabilities resulting from the different alternatives for the San Andreas fault. The probabilities based on the alternatives were combined following established procedures (appendix B) to arrive at the final consensus probabilities. In appendix C, we also report quantitative confidence limits to provide a measure of the range of probabilities permitted by the parametric uncertainty.

The probabilities of large–magnitude earthquakes considered in this report constitute a hypothesis that will either prove to be viable or will be rejected in the coming years. Parameters relevant to the success or failure of these forecasts principally relate to the timing, location, and length of rupture. Secondary parameters such as the amount of fault slip and derivative parameters such as earthquake magnitude are inherently less well defined in these forecasts.

Segment boundaries have been chosen on the basis of whatever seismic, geologic, and geodetic evidence is available. Different pieces of evidence usually agree to within 5–10 km, and on this basis we estimate an uncertainty of rupture boundaries of about ±10 km (± values represent estimates of one standard deviation). We would consider a segment forecast to be successful if more than 50 percent of the segment ruptured during an earthquake.

The relation between the surface expression of a fault and the actual fault surface at depth may be complex. An example of this is given by evidence of the complex three–dimensional structure of the aftershock zone and the diversity of aftershock focal mechanisms of the Loma Prieta earthquake (Dietz and Ellsworth, 1990). Experience from the Loma Prieta earthquake and mismatch between the 1984 Morgan Hill earthquake and the surface trace of the Calaveras fault lead us to estimate the horizontal uncertainty of a segment, measured perpendicular to the fault trace, to be about

± 2.5 km. Extreme variations of ± 5 km may occur in mountainous regions where complex fault zones that include nonvertical faults with significant dip–slip components of motion are common.

Uncertainties in segmentation also apply to the depth interval that produces the earthquake. On those segments with microearthquakes, the maximum depth of significant microseismicity marks the probable lower depth limit of earthquake rupture (Sibson, 1984). For the San Andreas fault segments considered here, we estimate the maximum depth of rupture to be 17 ± 3 km, and for the Hayward and Rodgers Creek faults, we estimate it to be about 12 ± 3 km. The upper limit of rupture is problematical. Where the fault shows no evidence of surface creep, an upper limit of 2 ± 2 km is suggested. For fault segments that are creeping at the surface, the upper limit of earthquake rupture may vary from the surface to the maximum depth of creep.

The amount of slip has not been explicitly considered. Rather we assign moment magnitudes based on segment length and the empirical length–displacement relation ($D = 2.8 \times 10^{-5} L$) employed by the previous 1988 Working Group. We emphasize that the slip values used to establish $\hat{T}$ are not predictive values for the next earthquake. When we combine the uncertainties estimated above with a 50–percent uncertainty in slip in the next event, we obtain an estimate of the uncertainty of about ± 0.3 moment magnitude units. Because the forecasts in this report are for strike–slip earthquakes and because significant dip–slip motion may sometimes occur (as in the case of the Loma Prieta earthquake), the displacement estimates and resulting magnitude estimates apply only to the strike–slip component of faulting.

SAN ANDREAS FAULT

Data relating to the assessment of earthquake probabilities for the San Andreas fault from San Juan Bautista to San Francisco permit a number of alternate interpretations that affect the calculation of earthquake probabilities. Although the Loma Prieta earthquake of October 17, 1989, has provided important new information for this section of the fault, it has not narrowed the number of permissible interpretations. Below, we review the interpretations employed in the 1988 Working Group report in the context of the Loma Prieta earthquake. Following this we discuss the different possibilities that arise in evaluating the segmentation of the fault and in the estimation of median recurrence times.

Depending upon choices made at each step in the evaluation, these alternate interpretations result in different outcomes for earthquake probabilities. Because the Working Group considered several alternatives to have significant merit, we have employed a "logic tree." A logic tree is a formalism that permits quantitative incorporation of the principal uncertainties into our final consensus evaluation of the San Andreas fault. At each decision point in the analysis, branches are added representing the principal alternatives. The analysis continues in parallel along each branch which in turn repeatedly branches as additional decision points are encountered. A probability is associated with the tip of each branch of the tree. The probability results from the series of choices leading to that particular tip. To arrive at a final consensus probability, the branchings at every decision point are assigned weights (that add up to 1.0) based on the judgment of the Working Group. The weight of a probability at a tip is the product of the branch weights leading to that tip. The final probability is the sum of the individual weighted probabilities. At the end of this section on the San Andreas fault, we summarize the consensus probabilities resulting from the logic tree analysis. Details of the logic tree analysis are presented in appendix B.

LOMA PRIETA EARTHQUAKE

The Loma Prieta earthquake of October 17, 1989, was located along the southern portion of the 1906 earthquake break in the southern Santa Cruz Mountains (fig. 2). The earthquake rupture, as deduced from the aftershock distribution and geodetic measurements of the coseismic deformation, initiated at a point 18 km beneath the surface and broke upward to within 4 to 6 km of the surface

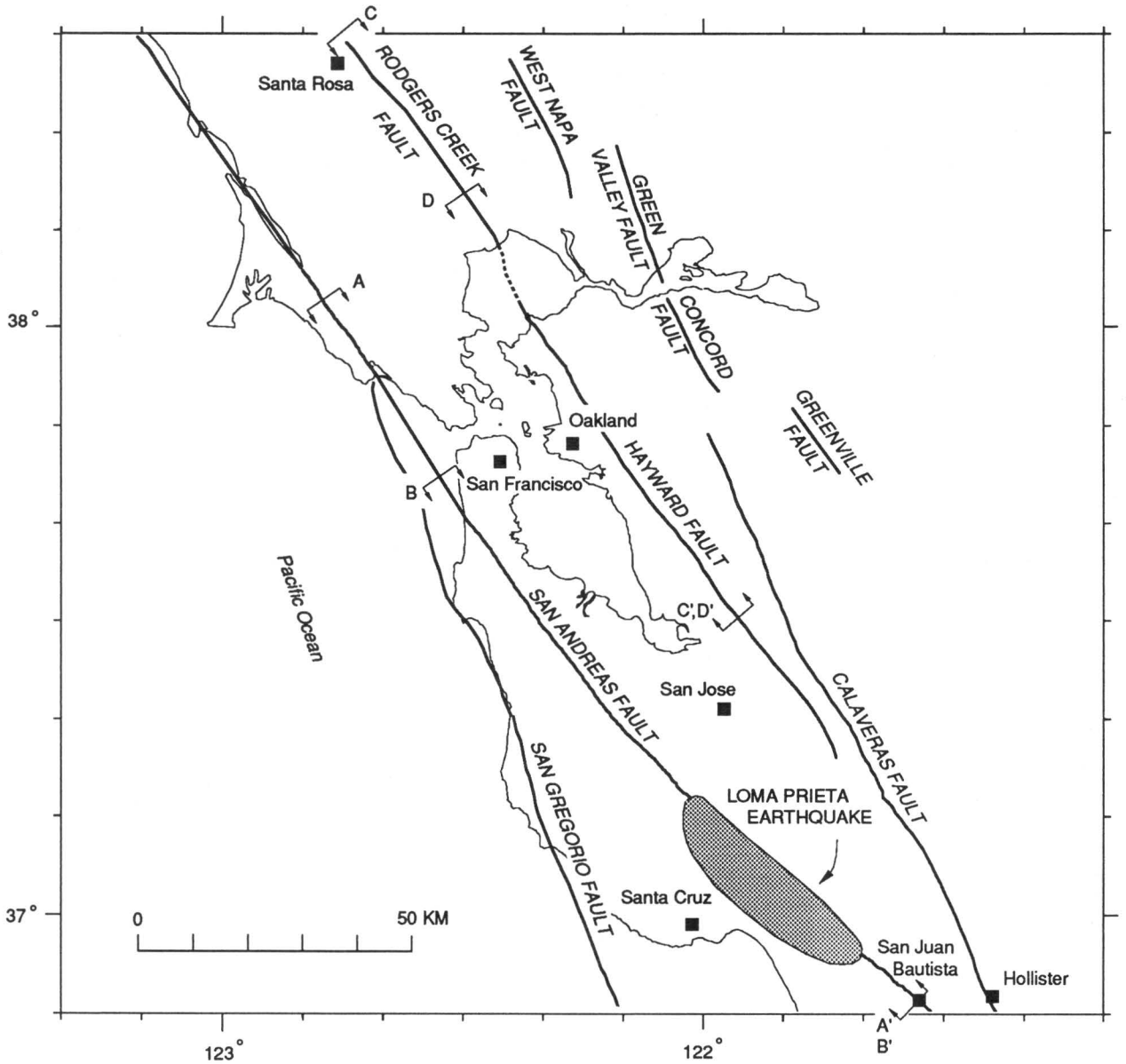

Figure 2. Major faults of San Francisco Bay region (dotted where inferred). Shaded area shows approximate aftershock area of October 17, 1989, Loma Prieta earthquake. A-A′, B-B′, C-C′, and D-D′ are endpoints of cross sections shown in figures 3, 4, 7, and 8, respectively.

(fig. 3). It did not produce a surface break. The rupture extended along strike for 35 to 40 km and involved right–reverse slip on a plane dipping 70° to the southwest. Preliminary dislocation models of the source based upon geodetic data indicate 1.6 ± 0.3 m of right–lateral strike–slip displacement and 1.2 ± 0.4 m of reverse slip (Lisowski and others, 1990). Details of the distribution of slip with depth and along strike are not available at this time.

A number of studies have considered the long–term seismic potential for the part of the San Andreas fault assumed to have ruptured in the Loma Prieta earthquake (Lindh and others, 1982; Lindh, 1983, 1988; Sykes and Nishenko, 1984; Scholz, 1985; Thatcher and Lisowski, 1987). These studies assumed slip rates varying from 12 to 20 mm/yr and also differed significantly in

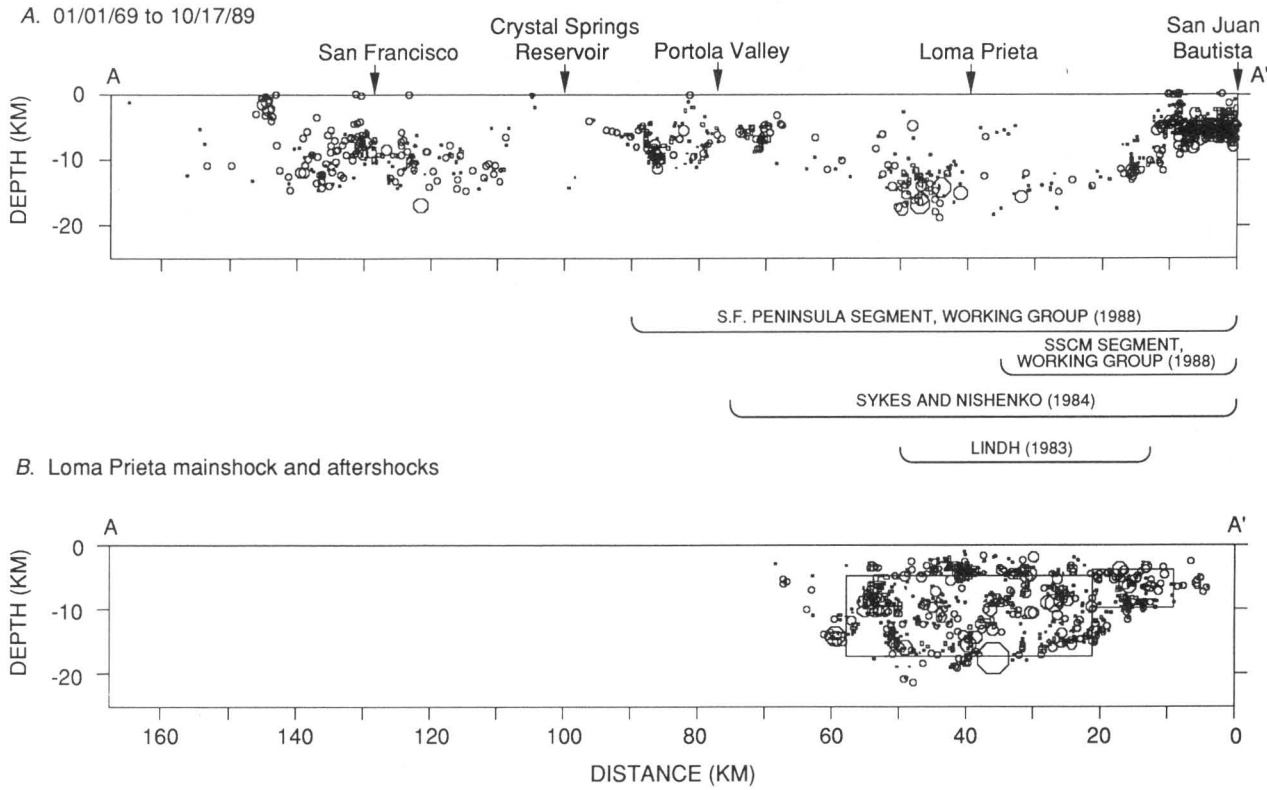

Figure 3. Seismicity along San Andreas fault, 1969-1989. *A*, seismicity before Loma Prieta earthquake, and *B*, aftershocks of Loma Prieta earthquake. Size of symbols increases with increasing magnitude. Bars below section *A* indicate location of fault segment forecasts discussed in text; southern Santa Cruz Mountains segment of Working Group (1988) is indicated by initials SSCM. Rectangles in section *B* give location of Loma Prieta earthquake rupture inferred from geodetic data (Lisowski and others, 1990). Locations of section endpoints, A-A′, are shown in figure 2.

estimates of the amount of slip at seismogenic depths in the great earthquake of 1906. Lindh (1983, 1988) obtained a 30–year probability of 0.47, and Sykes and Nishenko (1984) obtained a 20–year probability of 0.19 to 0.95.

In 1988 the Working Group on California Earthquake Probabilities reassessed these probability estimates. Geodetic estimates of the 1906 earthquake slip distribution were relied on to divide the fault into segments and to constrain 1906 slip values used in the calculation of expected recurrence time. Two segments considered by the 1988 Working Group are relevant to the Loma Prieta earthquake. They are the San Francisco Peninsula segment (30–year probability of 0.2) and the southern Santa Cruz Mountains segment (30–year probability of 0.3). Although the southern Santa Cruz Mountains segment was assigned the highest probability in the region, a low level of reliability (E on the A–to–E scale used in the 1988 report) was attached to the probability estimate for that segment because seismic history and slip were not well defined.

The location and dimensions of the 1989 earthquake most closely correspond to the forecast of Lindh and others (1982) and Lindh (1983, 1988), but the magnitude was larger than anticipated (fig. 3). At M 7.1, it was close to the magnitude forecast by Sykes and Nishenko (1984) for a 75–km–long segment. The Loma Prieta earthquake occurred on parts of two segments defined by the 1988 Working Group: the southern Santa Cruz Mountains segment and the San Francisco

Peninsula segment. The Loma Prieta earthquake rupture is about the same length as the segment defined by the 1988 Working Group as the southern Santa Cruz Mountains segment, but the center of that segment is about 15 km to the south of the center of the earthquake rupture.

IMPLICATIONS OF THE LOMA PRIETA EARTHQUAKE

An important question is the extent to which slip in the 1989 earthquake represents recurrence of slip on this part of the 1906 rupture. If the 1906 slip observations apply to the source region of the Loma Prieta earthquake, then we may take 1906 as the appropriate previous event for interpreting the Loma Prieta earthquake and the various means of forecasting its occurrence. If, on the other hand, the 1989 earthquake source region moved little or not at all in 1906, then we may draw incorrect conclusions when 1906 is taken to be the prior rupture.

Present information is insufficient to definitively resolve this issue. The 1906 earthquake rupture extended at least as far south as the Loma Prieta earthquake rupture zone, as evidenced by the large displacement of the Loma Prieta triangulation bench mark and by faulting in the Wright–Laurel tunnel. However, we do not know how the 1906 fault displacement varied along strike, whether it reached the surface, where it terminated, if there was a reverse–slip component, or how it varied with depth. The geodetic observations of the 1906 earthquake only indicate that there were large (~2.5 m) right–lateral displacements from near the surface to a depth of 5 to 10 km at Loma Prieta (Thatcher and Lisowski, 1987). The data cannot be used to resolve the amount of slip at greater depths. Thus, the 1989 earthquake rupture probably overlaps at least some of the 1906 rupture below a depth of about 5 km, but could have significant differences in the depth distribution of slip.

It is also possible that the 1989 and 1906 slip occurred on different but closely spaced fault planes. Certainly the prominent thrust faulting component of the 1989 earthquake is unlikely to occur in every event. Along this part of the San Andreas fault zone there are other narrowly spaced fault strands, in particular the Sargent fault. However, the stress drop produced by the Loma Prieta earthquake is likely to have affected a sufficient volume of crust such that it makes little difference which of several closely spaced fault planes slipped. Acknowledging all of the uncertainties, the Working Group judges the currently available evidence to favor the interpretation that, for the purposes of this study, the 1989 earthquake represents recurrence of slip along the 1906 fault break.

The occurrence of the 1989 Loma Prieta earthquake, within two years of the publication of the 1988 Working Group's report, provides a test of prior interpretations and assumptions for this part of the San Andreas fault. Earlier estimates of recurrence time (Lindh and others, 1982; Lindh, 1983; Sykes and Nishenko, 1984; Scholz, 1985; Thatcher and Lisowski, 1987; Lindh, 1988; Working Group, 1988) differed significantly because of differences in assumed slip rate and 1906 displacement. The southern half of the Loma Prieta earthquake rupture was within the southern Santa Cruz Mountains segment, which was assigned a 1906 fault slip of 200 ± 50 cm by the Working Group (1988). The northern half of the Loma Prieta earthquake rupture was within the San Francisco Peninsula segment, which was assigned a 1906 slip of 250 ± 60 cm based on displacement of the Loma Prieta triangulation benchmark. These displacements divided by the assumed slip rate of 16 ± 2.5 mm/yr yield estimates of median recurrence time, $\hat{T}$, of 125 years for the southern Santa Cruz Mountains segment and 156 years for the San Francisco Peninsula segment. Does the occurrence of the Loma Prieta earthquake only 83.5 years (1906.3–1989.8) after the most recent earthquake "disprove" the Working Group (1988) recurrence estimates?

A statistical hypothesis test can be constructed. The Working Group (1988) not only estimated recurrence time intervals, they also stated their then–current uncertainty in recurrence time through the parameter σ_P and included the effect of σ_P in their probability estimates. Therefore, a hypothesis test of their stated position should be based on the (log) observed recurrence time (83.5 years), (log) median recurrence time estimate, $\hat{T}$, (125 or 156 years), and their total

uncertainty,[3] σ_N (=0.36). Specifically, one should reject the 1988 committee's hypothesis if

$$\ln (83.5) < \ln \hat{T} - \lambda \sigma_N, \tag{4}$$

in which λ characterizes the significance level of the test (1.96 and 1.65 for a significance level of 1 percent and 5 percent, respectively). The conclusion is that we can accept either the 125–year or 156–year hypothesis for $\hat{T}$ at the 1–percent significance level, whereas at the 5–percent level one may accept the 125–year estimate but should reject the 156–year estimate. In short, the observed 83.5–year recurrence interval is consistent with the 1988 Working Group's statements, although only marginally so with respect to the segmentation interpretation that yielded the 156–year estimate.

On the other hand, after the event, given the "closed interval" of 83.5 years, the uncertainty of the log of the hypothesized median is no more than[4] $\sigma/\sqrt{n}$, where n is the sample size (here, $n = 1$). In this case, one can reject any mean that might be hypothesized whose (log) median is

$$\ln \hat{T} < \ln (83.5) + \lambda\sigma\sqrt{n}. \tag{5}$$

For $\sigma = 0.21$, $n = 1$, and $\lambda = 1.65$ (or 1.96), this value of $\hat{T}$ is 118 years (or 126 years).

In this sense, the 1988 Working Group estimates of $\hat{T}$ were somewhat large. The method of estimating $\hat{T}$ for segments of the San Andreas fault north of San Juan Bautista relied on interpretations of 1906 displacements and fault slip rate similar to those employed for the Loma Prieta section of the fault. Consequently, if the 1988 Working Group overestimated the recurrence time for the section of the San Andreas fault that ruptured in the Loma Prieta earthquake, then recurrence times for other segments of the San Andreas fault north of San Juan Bautista may also have been overestimated.

1906 EARTHQUAKE SLIP DISTRIBUTION

Figure 4 summarizes fault slip information for the great $M\sim8$ earthquake of 1906 from San Juan Bautista to Mussel Rock. These data are from observations of surface fault offsets (Lawson, 1908) and modeling of geodetic observations (Thatcher and Lisowski, 1987) based on triangulation measurements made prior to and following the earthquake (Hayford and Baldwin, 1908). Surface fault offsets provide point observations of slippage. Because offset features seldom span the entire zone of earthquake slip and because distributed deformation is possible in near–surface materials, surface offsets often represent lower bounds to the total slip at depth. In principle, the geodetic observations reflect the total earthquake slip at depth, over large areas of the fault surface and across the full width of the fault zone. However, slip distribution from the geodetic observations must be inferred from modeling, which introduces its own uncertainties. Geodetic slip on the segment centered near Mussel Rock is estimated from observations at Mt. Tamalpais (not shown in fig. 4), which is about 20 km northwest of Mussel Rock.

Northwest of Crystal Springs Reservoir (109 km on fig. 4) the surface fault offset values show considerable scatter, but their maximum values of 4 to 5 m are consistent with the geodetic estimates. For this segment (part of the North Coast segment) the previous Working Group used a slip value of 4.5 ± 0.5 m. Farther to the southeast the surface offset data are sparser and give maximum values that are considerably less than those determined geodetically. Between Crystal Springs and Woodville (now Woodside) the two available surface offset values are about 2.3 m, whereas the geodetic estimates are between 3.1 and 3.4 m. Southeast of Page Mill Road the lowest geodetic slip estimate is 2.3 ± 0.2 m and the largest surface offset is 1.5 m. The previous Working

[3] The net uncertainty values given in table 1 of the 1988 report are erroneously stated. However, the correct values were used in the calculation of probabilities stated in that report.

[4] See equation 8.

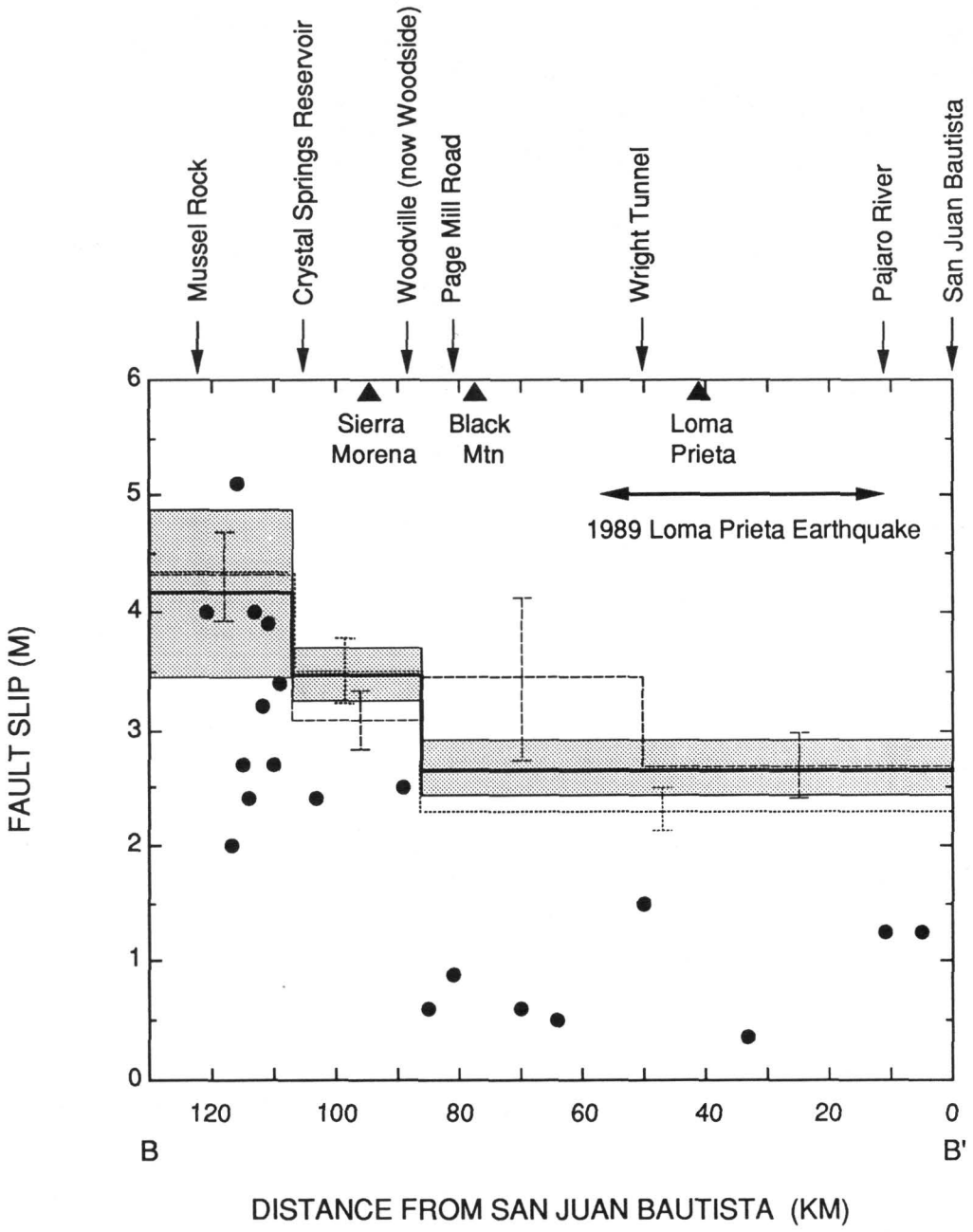

Figure 4. Geodetically estimated 1906 coseismic slip (lines) and surface fault offsets (dots) along San Andreas fault. Endpoints of plot, B-B′, are shown in figure 2. Triangles at top of figure project location of three important benchmarks. Solid line shows fault-slip model from Thatcher (1975), with one-standard-deviation error (stippled areas). Dotted line shows model calculation in which all observations made prior to about 1880 have been deleted. Dashed line plots slip distribution obtained when additional fault segment centered near Black Mountain is included in fault model (Thatcher and Lisowski, 1987). Dotted and dashed vertical bars show one-standard-deviation error. Horizontal arrow shows inferred extent of rupture in the 1989 Loma Prieta earthquake.

Group used slip values of 2.5 ± 0.6 for the San Francisco Peninsula segment and 2.0 ± 0.5 for the southern Santa Cruz Mountains segment at the south end of the 1906 rupture.

SAN ANDREAS FAULT SLIP RATE

Sources of information for estimating the slip rate along the San Andreas fault include the record of large historical earthquakes, ages of offset geological features, and geodetic observations of displacement rates near the San Andreas fault. Interpretation of each data set is currently subject to uncertainty. Slip rate estimates are summarized in table 1.

Geological studies give slip rates generally in the range of 10 to 25 mm/yr. These rates tend to be lower than some other estimates, but it should be noted that geologic slip rates are subject to the same limitations as the geologic observations of 1906 slip and tend to underestimate the full slip rate. On the San Francisco Peninsula, a 28–km offset of the 1– to 3–million–year–old gravels of the Santa Clara Formation gives a slip rate of 10 to 30 mm/yr (Cummings, 1968). A later study by Cummings (1983), of another facies of the Santa Clara Formation, found roughly 3–km offset of 0.45–million–year–old gravels indicating a slip rate of about 8 mm/yr. Offset of units 1.8 to 5 million years old gives a slip rate of 6 to 22 mm/yr (Addicott, 1969). Near Lake San Andreas, Hall (1984) dated a Holocene offset of a stream channel, which yielded a minimum slip rate of 12 mm/yr. The trench at this site was recently reopened (N.T. Hall, written commun., 1990) in hope of obtaining better constraints on the slip rate. Seven charcoal samples from the horizon used to develop the original slip rate were dated and gave a range of 1,800 to 2,800 ^{14}C years before present. This age range results in a reduction of the minimum geologic slip rate to 7.5 mm/yr for the past 1,800 years. Finally, at Point Arena, 200 km to the north of San Francisco, a study of offset terraces by Prentice (1989) yielded an upper limit for slip rate of about 25 mm/yr for the San Andreas fault.

Geodetic measurements provide detailed data on the short–term strain rates in the vicinity of the San Andreas fault, but interpretations of those observations to infer slip rates currently have considerable uncertainty. Prescott and others (1981) report a lower–bound slip rate of 12.2 ± 4 mm/yr (the net displacement rate across a 40–km–wide zone centered on the San Andreas fault). Dislocation model inversions of the data by Prescott and others (1981), assuming deep slip at a constant long–term rate with the upper 10 km of the fault locked, yield 21.5 mm/yr. Prescott and others (1981) do not report a preferred value, but W.H. Prescott (written commun., 1990) prefers a slip rate of about 15 mm/yr. Block motion inversion for San Andreas slip in the vicinity of San Juan Bautista gives a rate of 13 mm/yr (Savage and others, 1979). However, simultaneous dislocation inversions for slip rate on the Hayward, Calaveras, and San Andreas faults yield slip rates of 22 to 26 mm/yr (Savage and others, 1979; Matsu'ura and others, 1986) for the San Andreas fault at San Juan Bautista and to the north. Geodetic estimates based on rigid block inversion are uncertain because the models are incapable of representing internal (elastic) deformation of the crust, while dislocation inversions are uncertain because of tradeoffs between deep slip rate and depth distribution of slip.

The occurrence of four large earthquakes in historical time (1838, 1865, 1906, 1989) suggests relatively large slip rates for the San Francisco Peninsula part of the San Andreas fault. The section of the fault affected by the 1989 Loma Prieta earthquake ($D = 1.6 \pm 0.3$ m) may have slipped previously in the earthquakes of 1906 and 1865. Estimates of 1906 slip vary from 1.5 to 2.6 m (fig. 4). The earthquake of October 8, 1865, may constitute an earlier rupture along this segment, but information pertaining to that earthquake is very limited. Isoseismals center the 1865 earthquake on the San Andreas fault at a location corresponding to the Loma Prieta earthquake and have been used to give an assigned magnitude of 6.3 (Toppozada and others, 1981) and 6.5 (Moths and others, 1981; Ellsworth, in press). Both magnitude and location are subject to great uncertainty, and it must be recognized that this earthquake may have occurred on an altogether different fault. Slip in 1865 is unknown, but the estimated magnitude of this event and the similarity

Table 1. San Andreas and southern Calaveras fault slip rate information

Source	Slip rate (mm/yr)	Description
		San Andreas fault slip rate, San Francisco Peninsula
Addicot (1969)	6–22	Geologic–Offset of 1.8 to 5.0 million–year old units.
Cummings (1968)	10–30	Geologic–Offset of 1.0 to 3.0 million–year–old units.
Cummings (1981)	8	Geologic–Offset of 0.45 million–year–old unit.
Hall (1984, 1990)	>12, >7.5	Geologic–Holocene offset of stream channel.
Prescott and others (1981)	12.2±4 21.5±1.3	Geodetic–Net rate across a zone 40 km wide. Not an inversion. Geodetic–2D dislocation inversion for deep slip rate, with fault locked to 10 km. Locking to 5 km and 20 km gives slip rates of 13.3±0.8 and 35.9±2.2, respectively.
Matsu'ura and others (1986)	26±3	Geodetic–Simultaneous inversion, deep slip rate on Hayward, Calaveras, and San Andreas faults.
Savage, written commun. (1990)	26–32	Geodetic–Deep slip rate with fault locked to depths of 13–16 km from 2D dislocation fit to observed 0.3 μstrain/yr of small-aperture geodetic networks.
		San Andreas fault slip rate, San Juan Bautista area
Savage and others (1979)	13±2 22.2±3.1	Geodetic-Inversion assuming rigid block motion of San Andreas and Calaveras faults. Geodetic–Simultaneous inversion, deep slip rate on Hayward, Calaveras, and San Andreas faults.
Mats'ura and others (1986)	25±3	Geodetic–Simultaneous inversion, deep slip rate on Hayward, Calaveras, and San Andreas faults.
		San Andreas fault slip rate, central creeping zone
Thatcher (1979)	33±1 38±3	Inversion assuming rigid block motion. Deep slip for slip below 15 km. Inversion for deep slip below 10 km gives 33±2.
Matsu'ura and others (1986)	37±2	Geodetic–Simultaneous inversion, deep slip rate on Hayward, Calaveras, and San Andreas faults.
		Southern Calaveras fault slip rate
Nason (1971)	15	Observed surface creep rate.
Savage and others (1979)	17±2 14.4±2.2	Inversion–assuming rigid block motion of San Andreas and Calaveras faults. Geodetic–Simultaneous inversion, deep slip rate on Hayward, Calaveras, and San Andreas faults. Solution for shallow creep rate is 14.9±1.8.
Matsu'ura and others (1986)	13±2	Geodetic–Simultaneous inversion, deep slip rate on Hayward, Calaveras, and San Andreas faults.

between its effects and those of the 1989 Loma Prieta earthquake, including liquefaction in San Francisco (Townley and Allen, 1939), are consistent with displacements of 1 to 2 m. Dividing the average displacement in these three earthquakes by the average interval between them yields a rough estimate of slip rate of about 25 mm/yr. Ignoring the 1865 event and assuming that the 1906 earthquake ruptured the same part of the fault plane that slipped in 1989, 1.6 ± 0.3 m of lateral slip was accumulated and released in 83 years. This yields a slip rate of 19 mm/yr.

Finally, constraints on slip rate may be derived by partitioning the total slip rate across the San Andreas system among the major faults of the San Francisco Bay region. The southern Monterey Bay geodetic profile spans most of the deformation zone and gives a net displacement rate of 38 ± 3 mm/yr (W.H. Prescott and M. Lisowski, written commun., 1990). Allowing for the possibility of some additional deformation beyond the ends of the profile, the total displacement rate could be as much as 40 mm/yr. Other estimates of total slip rate in the creeping section of the San Andreas fault south of Hollister vary from 33 to 37 mm/yr (table 1). North of Hollister, the total slip appears to be partitioned between the southern Calaveras and San Andreas faults. To the north, closer to San Francisco Bay, the southern Calaveras fault slip is believed to feed onto the Hayward, northern Calaveras, and possibly other faults to the east. If the total slip is partitioned among the Hayward, Calaveras, and San Andreas faults, then we may use the data from the southern Calaveras fault, which is creeping, to bound the slip rates on the east and west San Francisco Bay faults. One estimate of creep rate on the southern Calaveras fault, 15 mm/yr, comes from Nason (1971) for a location 13 km north of Hollister. This is consistent with southern Calaveras slip rates inferred from inversions of geodetic data that give 13–17 mm/yr (table 1). Subtracting the 15 ± 2 mm/yr southern Calaveras rate from the 38 ± 3 mm/yr total rate of slip across the San Andreas system leaves an upper-bound estimate of 23 ± 4 mm/yr for the rate of slip on the San Andreas fault. However, some unknown portion of this deformation rate may be taken up by slip on faults to the west of the San Andreas, such as the San Gregorio fault, or by bulk shear across the San Francisco Bay region.

In light of these considerations, the current Working Group concluded that the previous estimate of 16 ± 2.5 mm/yr was probably too small. The Working Group has adopted a slip rate of 19 ± 4 mm/yr for estimation of revised recurrence times.

SEGMENTATION

The southern Santa Cruz Mountains segment has been redefined to coincide with the primary rupture zone of the 1989 Loma Prieta earthquake. This moves the segment boundaries about 15 km north from the locations used in the 1988 report. On the basis of the aftershock distribution in the first 3 hours following the mainshock and the results of analyses of geodetic data (Lisowski and others, 1990), the segment length is taken as 39 km. The segment extends from just north of the intersection of the San Andreas fault and Highway 17, between San Jose and Santa Cruz, south to Pajaro Gap, 15 km northwest of San Juan Bautista.

Two alternatives for segmentation of the San Francisco Peninsula part of the San Andreas fault have been considered (fig. 5). The first is a single segment (San Francisco Peninsula) that extends 60 km from the vicinity of Lower Crystal Springs Reservoir to the northern end of the redefined southern Santa Cruz Mountains segment. This segment may correspond to the location of the $M{\sim}7$ earthquake of 1838 (Lindh, 1983). The second alternative divides the San Francisco Peninsula segment into two segments: the northern Santa Cruz Mountains segment and the mid–Peninsula segment. The mid–Peninsula segment extends from Lower Crystal Springs Reservoir about 40 km south to the intersection of Page Mill Road and the San Andreas fault. The northern Santa Cruz Mountains segment extends 20 km from Page Mill Road to the northern end of the southern Santa Cruz Mountains segment. North of the San Francisco Peninsula segment, the North Coast segment of the 1988 Working Group has been retained.

Segment boundaries of the southern Santa Cruz Mountains segment are fixed by the Loma Prieta earthquake rupture. For the remaining two segment boundaries, the evidence of fault geometry, seismicity, and 1906 slip distribution, summarized below and in figures 3, 4, and 5, was considered. Coordinates of the segment boundaries are listed in table 2.

Several notable changes in fault strike occur along the 120-km-long section of the San Andreas fault from Mussel Rock to San Juan Bautista (fig. 5). The most prominent feature is a 9° change in strike located at Black Mountain that was noted by Scholz (1985). This bend marks the

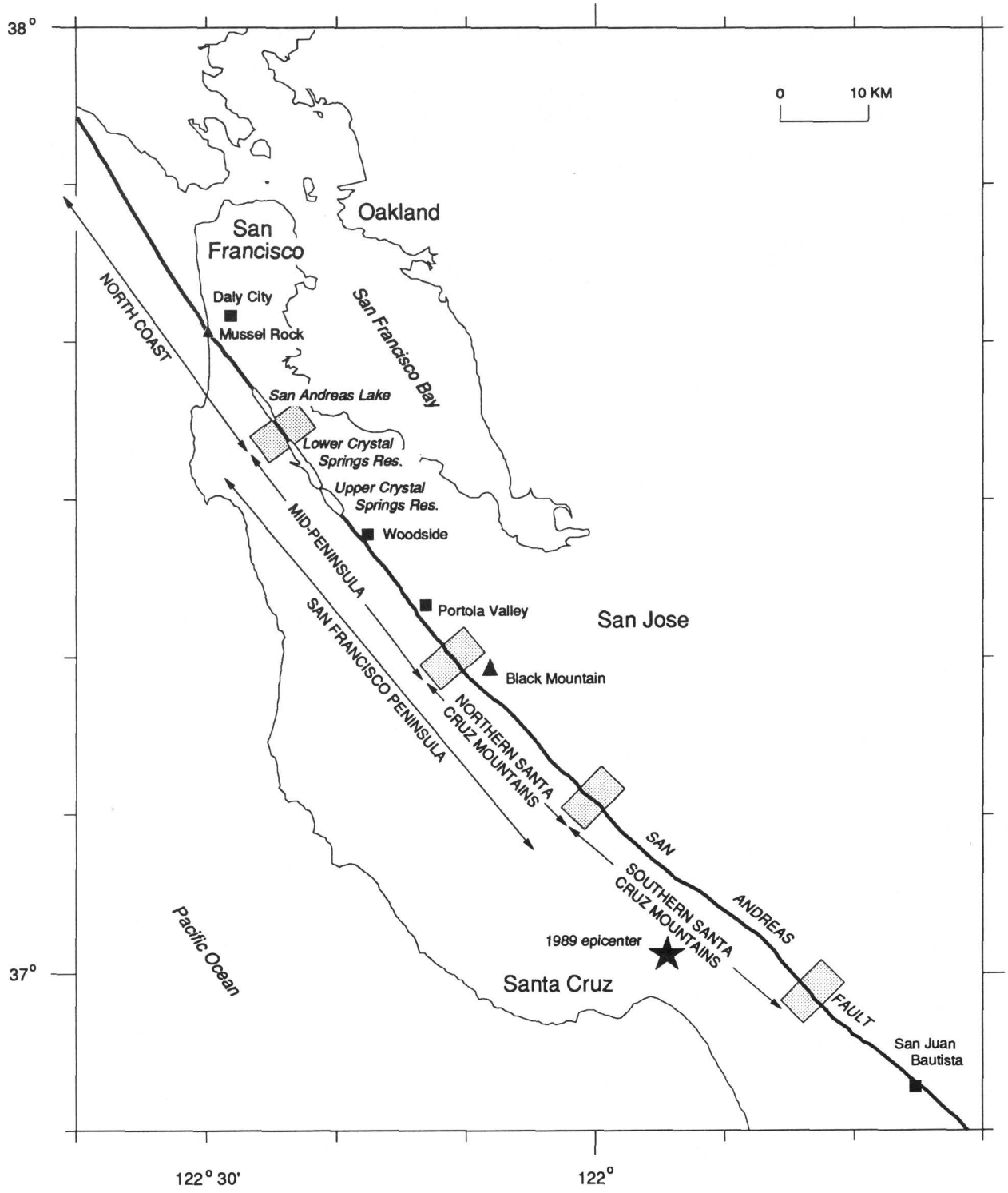

Figure 5. San Andreas fault segments. Stippled rectangles are segment boundary zones. Star marks epicenter of 1989 Loma Prieta earthquake.

approximate location of the north end of the northern Santa Cruz Mountains segment and the southern end of the mid–Peninsula segment. There are two additional changes in fault trend of about 8° (see also Nishenko and Williams, 1985). A smaller, approximately 5° change in trend occurs near Lower Crystal Springs Reservoir, where the reverse-slip Canada fault intersects the San Andreas.

Table 2. San Andreas fault segments

Segment	Coordinates of segment boundaries[1] Northwest end Lat. (N.)	Long. (W.)	Southeast end Lat. (N.)	Long. (W.)	Length (km)	Expected magnitude
Southern Santa Cruz Mountains	37°12′	122°01′	36°58′	121°44′	39	7
Northern Santa Cruz[2] Mountains	37°20′	122°11′	37°12′	122°01′	20	6.5
Mid–Peninsula[2]	37°34′	122°24′	37°20′	122°11′	41	7
San Francisco Peninsula	37°34′	122°24′	37°12′	122°01′	61	7
North Coast	40°17′	124°30′	37°38′	122°01′	340	8

[1] Coordinates correspond to midpoints of stippled rectangles in figure 5.
[2] Subsegments of the San Francisco Peninsula segment.

A seismicity gap on the San Andreas fault extends from the 1989 aftershock zone northwest to the vicinity of Crystal Springs Reservoir, interrupted only by small clusters of activity near Portola Valley (Olson, 1986; fig. 3). The northern end of the San Francisco Peninsula and mid–Peninsula segments corresponds approximately to the clear discontinuity in 1906 slip that is evident from both the geologic and geodetic observations (fig. 4).

RECURRENCE TIMES

Prior to the Loma Prieta earthquake the median recurrence times, $\hat{T}$, could only be estimated for San Andreas fault segments from the ratios of the estimated 1906 slip to the estimated slip rate. The Loma Prieta earthquake brings new information to the assessment of the San Andreas fault along the San Francisco Peninsula that may modify earlier estimates of $\hat{T}$. Now that this segment has ruptured, the single datum we know best is the inter–event time of 83 years, assuming of course, that this segment ruptured in the 1906 earthquake. How then does this new information change our perception of the earthquake potential of this segment and of the other segments? The Working Group has considered three alternatives for estimation of recurrence times. In the following, we refer to these alternatives as recurrence time models 1, 2, and 3. Recurrence time estimates and earthquake probabilities from these three models have been incorporated into the logic-tree analysis. Results of the estimation of recurrence time using the three approaches are summarized in table 3.

Model 1 retains the conclusions of the 1988 Working Group report with modifications based only on changes in segmentation. This alternative holds that no revision of the parameters is warranted by the occurrence of the Loma Prieta earthquake. It is based on the postulate that the Loma Prieta earthquake represents an example of vertical segmentation, in which slip on a shallow 1906 rupture has not recurred. Recurrence time is obtained from the time–predictable model (equation 3) using $V = 16 \pm 2.5$ mm/yr.

Model 2 combines the revised estimate of fault slip rate ($V = 19 \pm 4$ mm/yr) with revised displacement estimates in the time–predictable model to determine $\hat{T}$ for the San Andreas fault segments. The procedure for obtaining revised estimates of segment displacement employed a separate logic tree that is described in appendix B.

Model 3 asserts that the observed 83–year interval on the southern Santa Cruz Mountains segment is the most certain information we have and that it should therefore receive more weight

Table 3. Summary of San Andreas fault segment parameters

[$\hat{T}$, recurrence time; σ_P, parametric uncertainty; n.a., not applicable]

Model	Accept stress effect	$\hat{T}$ (years)	σ_P	Weight
Southern Santa Cruz Mountains segment (previous event=1989)				
1	n.a.	100±24	0.24	0.13
2	n.a.	84±24	.28	.47
3	n.a.	96±16	.17	.40
Northern Santa Cruz Mountains segment (previous event=1906)				
1	no	156±45	.28	.09
1	yes	127±45	.34	.04
2	no	95±44	.44	.31
2	yes	70±43	.56	.16
3	no	96±36	.37	.27
3	yes	71±43	.56	.13
Mid–Peninsula segment (previous event=1906)				
1	no	213±60	.27	.09
1	yes	210±60	.27	.04
2	no	129±49	.37	.31
2	yes	127±49	.38	.16
3	no	149±31	.21	.27
3	yes	147±30	.20	.13
San Francisco Peninsula segment (previous event=1906)				
1	no	188±54	.28	.02
1	yes	176±53	.29	.11
2	no	138±40	.28	.08
2	yes	128±38	.29	.39
3	no	138±29	.21	.06
3	yes	129±28	.21	.34
North Coast segment (previous event=1906)				
1	n.a.	281±76	.27	.13
2	n.a.	237±73	.30	.47
3	n.a.	201±49	.24	.40

in the revised estimation of $\hat{T}$ on San Andreas fault segments. Under this approach, all San Andreas fault recurrence–time estimates are obtained by reference to an updated estimate of the median recurrence time, $\hat{T}_{LP}$, for the southern Santa Cruz Mountains segment following 1906. The update is based on the Loma Prieta earthquake. The procedure compares the observations of 1906 displacement along the southern Santa Cruz Mountains segment with the 1906 displacement observations on the segment of interest. The recurrence time for a San Andreas segment (other than the southern Santa Cruz Mountains segment itself) is then

$$\hat{T} = \hat{T}_{LP} + \frac{\Delta D}{V}, \tag{6}$$

where ΔD is the difference between the 1906 displacement on the segment in question and the 1906 displacement on the Loma Prieta rupture, and V is the revised slip rate of 19 ± 4 mm/yr.

The updated estimate, $\hat{T}_{LP}$, appearing in equation (6) is found by application of Bayes theorem. Using the 1906 slip estimate of 2.5 ± 0.6 m (Working Group, 1988) and the revised slip rate of 19 ± 4 mm/yr gives the *a priori* expected recurrence time of 132 ± 42 years. Using Bayes theorem

with the observed interval of 83 years gives

$$\hat{T}_{LP} = \exp\left\{ \frac{\left[\frac{\log 132}{.31^2} + \frac{\log 83}{.21^2}\right]}{\left[\frac{1}{.31^2} + \frac{1}{.21^2}\right]} \right\} = 96 \pm 16, \tag{7}$$

in which the standard deviation, 16, is based on the revised parametric uncertainty in $\hat{T}_{LP}$:

$$\sigma_P = \sqrt{\frac{1}{\frac{1}{.31^2} + \frac{1}{.21^2}}} = 0.17. \tag{8}$$

The calculation of σ_P, the parametric uncertainty of log $\hat{T}$ from equation (6) is summarized in appendix B.

Southern Santa Cruz Mountains Segment

The prior event for this segment is now the 1989 Loma Prieta earthquake. Strike–slip displacement in the Loma Prieta earthquake is well constrained by the geodetic models to be 1.6 ± 0.3 m (Lisowski and others, 1990). Model 1 retains the earlier 16 mm/yr estimate of slip rate and gives $\hat{T} = 100 \pm 24$ years. The estimated San Andreas slip rate for model 2 is 19 mm/yr yielding $\hat{T} = 84 \pm 24$ years. With model 3, $\hat{T}$ for the post–1989 interval is taken as the revised estimate of 96 ± 16 years.

Northern Santa Cruz Mountains Segment

Between the northern end of the Loma Prieta earthquake rupture and Alpine Road, surface ruptures due to the 1906 earthquake were highly discontinuous, and right–lateral displacements nowhere exceeded the 1.5–m offset in the Wright–Laurel tunnel (Lawson, 1908). Similarly, although they are larger than the surface offsets, the geodetic estimates of displacement during the 1906 earthquake do not distinguish this segment from the southern Santa Cruz Mountains segment. Hence, model 1 assumes D=2.5±0.6 m on the basis of geodetic observations and V=16±2.5 mm/yr to obtain $\hat{T} = 156 \pm 46$ years. The consensus D for model 2 is 1.8 ± 0.7 m, which with $V = 19 \pm 4$ mm/yr gives $\hat{T} = 95 \pm 44$ years. Because 1906 displacements on this segment cannot be distinguished from those on the southern Santa Cruz Mountains segment, $\Delta D = 0.0 \pm 0.6$ m for model 3, and equation (6) gives $\hat{T} = 96 \pm 36$ years.

Mid–Peninsula Segment

This segment is about 40 km long and lies north of the northern Santa Cruz Mountains segment. From analysis of the geodetic observations, Thatcher and Lisowski (1987) gave their preferred slip of 3.4 ± 0.3 m for this section of the San Andreas fault. Surface offsets of 2.3 m or more were found at two sites, where it was noted that the fault trace was more continuous than farther to the south. For model 1, D is taken to be 3.4 ± 0.8 m, giving an estimated recurrence time, $\hat{T}$, of 213 ± 60 years. For model 2, D is taken as 2.46 ± 0.78 m, giving an expected recurrence time of 129 ± 49 years. In model 3, ΔD has been estimated to be 1.0 ± 0.3 m on the basis of the observation that 1906 slip (both surface and geodetic slip) on this segment was about 1.0 m greater than the slip on the southern Santa Cruz Mountains segment. This value results in an estimate for $\hat{T}$ of 149 ± 31 years.

San Francisco Peninsula Segment

This segment consists of the northern Santa Cruz Mountains segment and the mid–Peninsula segment combined. For this segment, model 1 uses a prior displacement, D, of 3.0 ± 0.7 m and model 2 uses $D = 2.62 \pm 0.52$ m. These values give expected recurrence times of 188 ± 54 years

for model 1 and 138 ± 40 years for model 2. In the case of model 3, ΔD has an assigned value of 0.8 ± 0.3, which results in an expected recurrence time of 138 ± 29 years.

North Coast Segment

This segment extends about 340 km north from the end of the San Francisco Peninsula segment. Maximum 1906 surface slip and geodetic displacements along this segment are in good agreement, and models 1 and 2 retain the previous Working Group estimate of 4.5 ± 0.5 m. This value gives expected recurrence times of 281 ± 76 years and 237 ± 73 years for models 1 and 2, respectively. Model 3 uses $\Delta D = 2.0 \pm 0.6$, giving $\hat{T} = 201 \pm 49$ years.

LOMA PRIETA EARTHQUAKE STRESSES

In addition to altering our perceptions of conditions along the San Andreas fault, the Loma Prieta earthquake may have caused a change of physical conditions that is sufficient to affect the time of earthquake rupture. In particular, slip on the Loma Prieta earthquake rupture surface has altered the stress on nearby fault segments. This stress change will bring a segment closer to the time of failure if the appropriate component of stress increased at the time of the earthquake or, conversely, will increase the time to failure if the stress decreased. As a consequence of the Loma Prieta earthquake we considered the possibility that the expected recurrence time was altered by ΔT, representing the equivalent change in recurrence time resulting from the Loma Prieta stress changes (Dieterich, 1988). We have incorporated this alternative into the logic-tree analysis so as to include an estimate of the physical effect of the Loma Prieta earthquake on recurrence times. This contrasts with the conventional approach, which does not provide for segment interactions.

The method assumes that the change of stress on a fault segment, $\Delta\tau$, resulting from slip on the Loma Prieta rupture surface is equivalent to the change of stress that would have occurred due to tectonic stressing at rate $\dot{\tau}$ in the interval ΔT:

$$\Delta T = -\Delta\tau/\dot{\tau}. \tag{9}$$

Hence, an increase of stress reduces the expected recurrence time. Three-dimensional elastic dislocation models of the San Andreas fault have been employed by R.W. Simpson and J.H. Dieterich (written commun., 1990) to estimate $\Delta\tau$ and $\dot{\tau}$ resulting from imposition of the geodetically determined Loma Prieta earthquake dislocation.

Because stressing rate is proportional to the slip rate ($\dot{\tau} = kV$), equation 9 is equivalent to

$$\Delta T = \frac{-\Delta\tau}{kV} = \frac{-D'}{V}, \tag{10}$$

where $D' = (\Delta\tau/k)$ is an equivalent reduction of the segment displacement, D, in the previous earthquake. Table 4 summarizes the results of R.W. Simpson and J.H. Dieterich (written commun., 1990) for D' and ΔT resulting from the Loma Prieta earthquake for San Andreas fault segments. The values in table 4 are based on the average change of stress over the entire segment. The Loma Prieta earthquake also changed the stresses along the Hayward fault, but because of the greater distances from the Loma Prieta earthquake, the stress effects are considered insignificant. The range of values for ΔT given in table 4 reflects the variation in ΔT resulting from different model assumptions and from the uncertainty of the Loma Prieta slip. Because of the rapid falloff of stresses with distance, the changes in recurrence time are greatest for the northern Santa Cruz Mountains segment, which is adjacent to the Loma Prieta earthquake rupture.

SUMMARY OF PROBABILITIES FOR THE SAN ANDREAS FAULT

Consensus probabilities, obtained from the logic-tree weights, are given in table 5. The low probability of an earthquake on the southern Santa Cruz Mountains segment, essentially zero in the

Table 4. Change of recurrence time resulting from simulated Loma Prieta earthquake studies

[See text for explanation of variables]

Segment	$D' = \Delta\tau/k$ (mm)	$\Delta T = D'/V$ (years) V = 16 mm/yr	V = 19 mm/yr
Mid–Peninsula	40±20	−2.5±1.3	−2.1±1.1
Northern Santa Cruz Mountains	470±230	−29.4±153	−24.7±13.3
San Francisco Peninsula	180±90	−11.3±6.9	−9.5±5.1

next 30 years, is based on our assumption that the earthquake of 1989 relieved stresses throughout the seismogenic depth along this section of the San Andreas fault zone. Because the 1989 Loma Prieta earthquake appears not to have slipped to as shallow a depth as apparently occurred in 1906, the possibility remains that the Loma Prieta earthquake did not relieve the stresses in the upper part of the seismogenic zone that have accumulated since 1906. This hypothesis is considered under model 1, which was given a low weight by the Working Group. If this hypothesis is correct, there may be a possibility for a shallow earthquake occurring above the 1989 Loma Prieta earthquake rupture. However, the maximum expected magnitude, 6 to 6.5, is below the magnitude range considered in this study.

The low probability of a $M\sim8$ earthquake on the North Coast segment (0.02) is the result of the large displacements, averaging about 4.5 m, that occurred along this segment in the great earthquake of 1906. The method we have employed considers only earthquakes that rupture the entire segment. However, slip information for the 1906 earthquake is somewhat sparse and subsegments of shorter length that had less than 4.5 m of slip in 1906 could have escaped detection. This possibility could not be evaluated, but it means that the North Coast segment, particularly north of Point Arena, could have a higher probability of producing smaller earthquakes of $M \leq 7$.

We considered two alternatives for the San Francisco Peninsula segment. The first, given a weight of 0.56, is that the entire segment will slip in an earthquake of about magnitude 7. The second scenario, given a weight of 0.44, is that separate earthquakes will rupture the northern Santa Cruz Mountains and mid–Peninsula subsegments of the San Francisco Peninsula segment. The expected magnitudes are 6.5 for the northern Santa Cruz Mountains segment and 7.0 for the longer mid–Peninsula segment. The sum of the San Francisco Peninsula segment probability multiplied by the segment weight (0.56), plus the mid–Peninsula segment probability times its weight (0.44), gives a 30–year probability of 0.23 for a magnitude 7 earthquake on this part of the San Andreas fault. The probability of a magnitude 6.5 earthquake on the northern Santa Cruz segment is the segment probability times the segment weight (0.44) and gives a 30–year probability of 0.18. Finally, considering both segmentation scenarios, the aggregate probability of a M 6.5 or M 7.0 event is 0.37 for the entire San Francisco Peninsula segment.

HAYWARD AND RODGERS CREEK FAULTS

HAYWARD FAULT ZONE

The previous Working Group identified and computed probabilities for two 50–km–long segments of the Hayward fault. New information on geologic slip rate, rates of historical surface creep, and segmentation provides a basis for revising the Hayward fault probabilities. Table 6 gives segmentation data, and table 7 summarizes parameters for calculations of probabilities for the Hayward and Rodgers Creek faults. Inputs for calculation of the probabilities in the 1988 Working Group report were (a) a 7.5 ± 2 mm/yr slip rate based on limited trenching data and regional geodetic interpretations, (b) a 1.4 ± 0.4 m slip per event, which was based on an empirical

Table 5. Probabilities of earthquakes along San Andreas fault

Segment	Previous event	Expected magnitude	Probability[1] 1990–2020	Level of reliability (scale of A to E; A most reliable)
S. Santa Cruz Mountains	1989	7	~0.00	B
N. Santa Cruz Mountains[2]	1906	6.5	.18	C
San Francisco Peninsula[3]	1906	7	.23	C
San Francisco Peninsula[4]	1906	6.5 or 7	.37	C
North Coast	1906	8	.02	B

[1] Differences in probability of less than 0.10 are not considered meaningful.
[2] Subsegment of San Francisco Peninsula segment. Probability incorporates weight for this segmentation scenario.
[3] Weighted average of San Francisco Peninsula segment and mid–Peninsula segment probabilities.
[4] Aggregated probability of *M* 6.5 or *M* 7 on San Francisco Peninsula segment.

Table 6. Hayward and Rodgers Creek fault segments

Segment	Coordinates of segment boundaries[1] Southeast end Lat. (N.)	Southeast end Long. (W.)	Northwest end Lat. (N.)	Northwest end Long. (W.)	Length (km)	Expected magnitude
Southern East Bay segment	37°30′	121°55′	37°44′	122°07.7′	32	7
Northern East Bay segment	37°44′	122°07.7′	38°07′	122°25′	50	7
Rodgers Creek fault	38°07′	122°25′	38°30′	122°45′	50	7

[1] Coordinates correspond to midpoints of stippled rectangles in figure 6.

relation between fault length and displacement, and (c) elapsed times of 120 and 162 years since the last earthquake for the south and north segments, respectively. The 30–year probability of a *M* 7 earthquake on each segment was previously calculated to be 0.2. Considering the uncertainties in the input parameters, the south segment (southern East Bay segment) probability was rated C and the north segment (northern East Bay segment) probability was rated D (Working Group, 1988).

The mode of strain accumulation along the Hayward fault presents a dilemma that cannot be resolved given our present state of knowledge. Two end–member hypotheses have been considered: (1) The fault is locked at depth (~5 to ~10 km) and accumulating strain at a rate appropriate to its long–term geologic slip rate, or (2) the fault is creeping and accumulating little or no elastic strain at present. The two alternatives clearly lead to divergent views of the earthquake hazard. The first hypothesis is consistent with the two major earthquakes on the fault in 1836 and 1868. The second is consistent with the high rate of surface creep. The committee carefully weighed both alternatives and various lines of evidence supporting them. The occurrence of surface creep in conjunction with documented *M* 6 to 7 earthquakes elsewhere on the San Andreas fault system (1979 Coyote Lake, 1966 Parkfield, 1979 Imperial Valley) argues for the locked–fault hypothesis. However, more data

Table 7. Hayward and Rodgers Creek fault segment parameters

[D, displacement in previous event; $\hat{T}$, recurrence time; σ_P, parametric uncertainty]

Segment	Slip rate $V = 9\pm2$ mm/yr Previous event	Expected magnitude	D (m)	$\hat{T}$ (years)	σ_P
Southern East Bay	1868	7	1.5±0.5	167±67	0.39
Northern East Bay	1836	7	1.5±0.5	167±67	.39
Rodgers Creek fault	1808 (or earlier)	7	2.0±0.5	≥222±74	.33

are needed to critically test this hypothesis, and new observations on the Hayward fault could well lead to significant revision (upward or downward) of the probabilities developed below.

Segmentation

The Hayward fault segmentation adopted for the present report is shown in figure 6. The stippled rectangles are segment boundary zones, and their along–fault width suggests the uncertainty in defining potential rupture endpoints. Coordinates of segment endpoints listed in table 6 correspond to the midpoints of the stippled zones.

We consider the fault to be composed of two fault segments. However, both segments appear to be well advanced in the earthquake cycle, and we recognize the possibility of both rupturing at the same time.

The extent of the southern East Bay segment is based on reports of the 1868 surface faulting (Lawson, 1908). In 1868, surface faulting was apparently well defined from Warm Springs to San Leandro and may have occurred discontinuously as far north as Mills College. This gives a segment length of 28 to 36 km. The south end of the segment coincides with increasing structural complexity of the fault zone and a change in the observed historical surface creep. Creep, which characterizes much of the Hayward fault as far north as San Pablo Bay, is not recognized south of Warm Springs. The north end of the segment is associated with an approximately 700– to 800–m–wide, 4–km–long right–stepping bend (a releasing bend), which is the most prominent geometric irregularity along this section of the fault. Coincident with the surface bend is an approximate doubling of the width of the zone of epicenters associated with the Hayward fault to a depth of about 10 km (D.H. Oppenheimer, written commun., 1989), suggesting that the releasing bend extends through the seismogenic zone. A cross section of seismicity along the Hayward and Rodgers Creek faults is shown in figure 7.

The northern East Bay segment is the section of fault between the 1868 rupture zone and the Rodgers Creek fault. It is a plausible location of the 1836 earthquake (Louderback, 1947; Toppozada and others, 1981). This segment has a length of 45 to 50 km. The south boundary is placed at the north end of the 1868 rupture zone (San Leandro–Mills College area). The north boundary is placed at the north side of San Pablo Bay where (a) there is a 6–km right (releasing) step to the Rodgers Creek fault at the surface (fig. 6), and (b) a well–defined 35–milligal negative Bouguer gravity gradient that characterizes this part of the Hayward-Rodgers Creek structural trend bends sharply northeast in the step–over area (Chapman and Bishop, 1988).

Slip Rate

An important change from the 1988 report is the Hayward fault slip rate. We have increased it from the previous value of 7.5 ± 2.0 mm/yr to 9 ± 2 mm/yr. This revision reflects new geologic data and new information on rates of historical surface creep. Trenching investigations near Union City

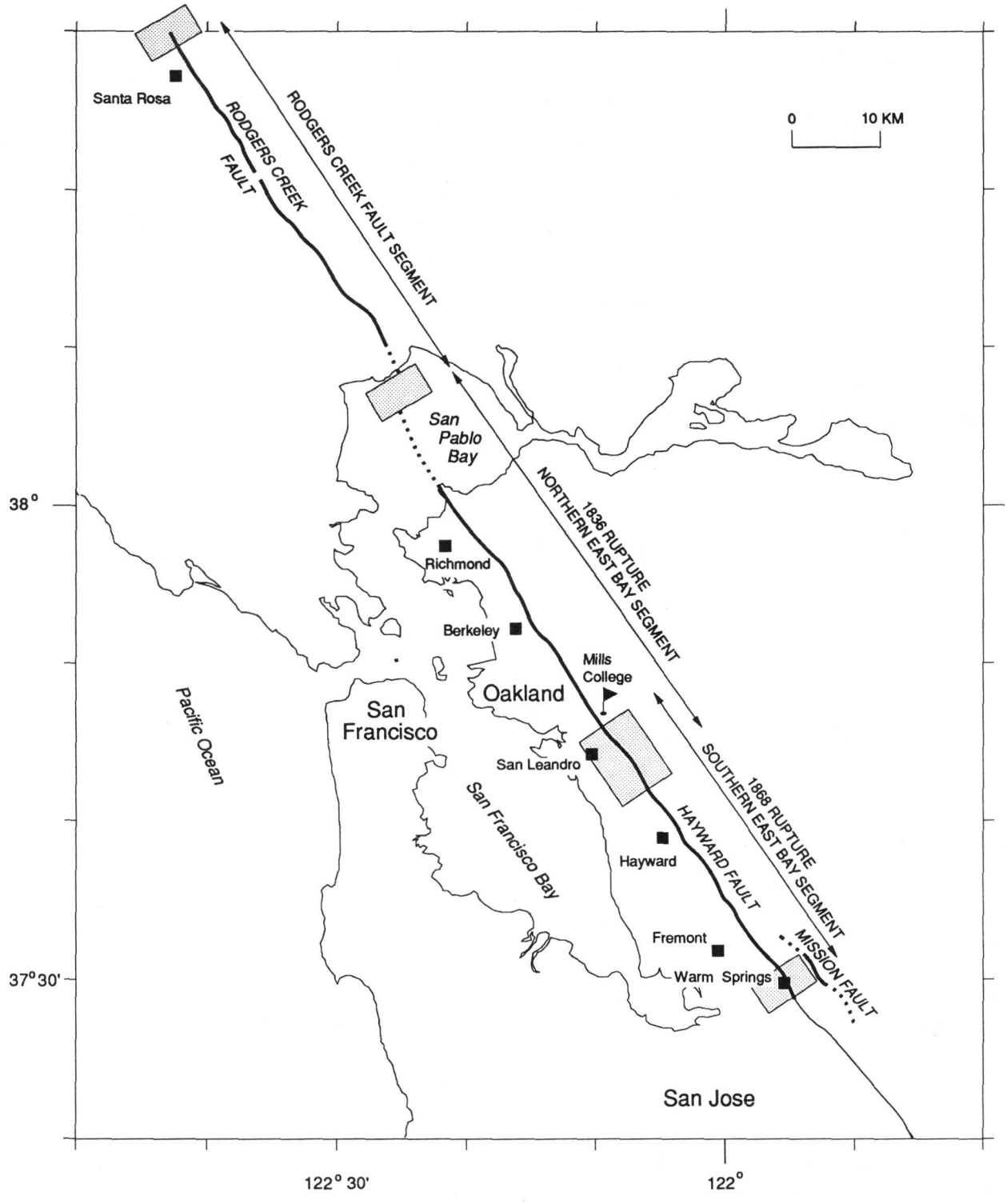

Figure 6. Hayward and Rodgers Creek fault segments. Faults dotted where inferred. Stippled rectangles are segment boundary zones; their along-fault width indicates relative uncertainty in defining segment endpoints.

(Lienkaemper and others, 1989) provide a preliminary estimate of 8 mm/yr for the past 8,000 years and permit a range of 7 to 10 mm/yr for periods between 4,000 and 14,000 years ago. Measurements of surface creep (fig. 8) (Lienkaemper and others, 1989) show that the Hayward fault has been

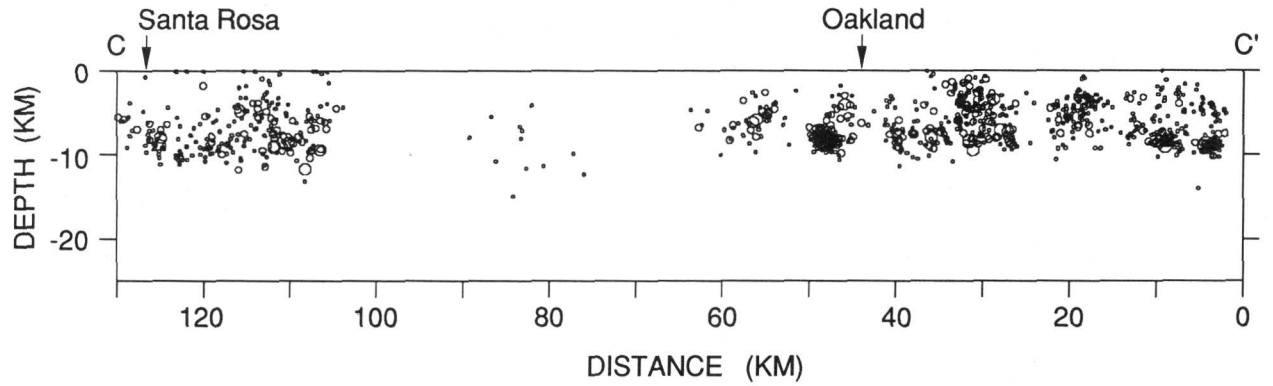

Figure 7. Seismicity along Hayward and Rodgers Creek faults, 1/1/69 to 1/31/90. Size of symbols increases with increasing magnitude. Locations of section endpoints, C-C′, are shown in figure 2.

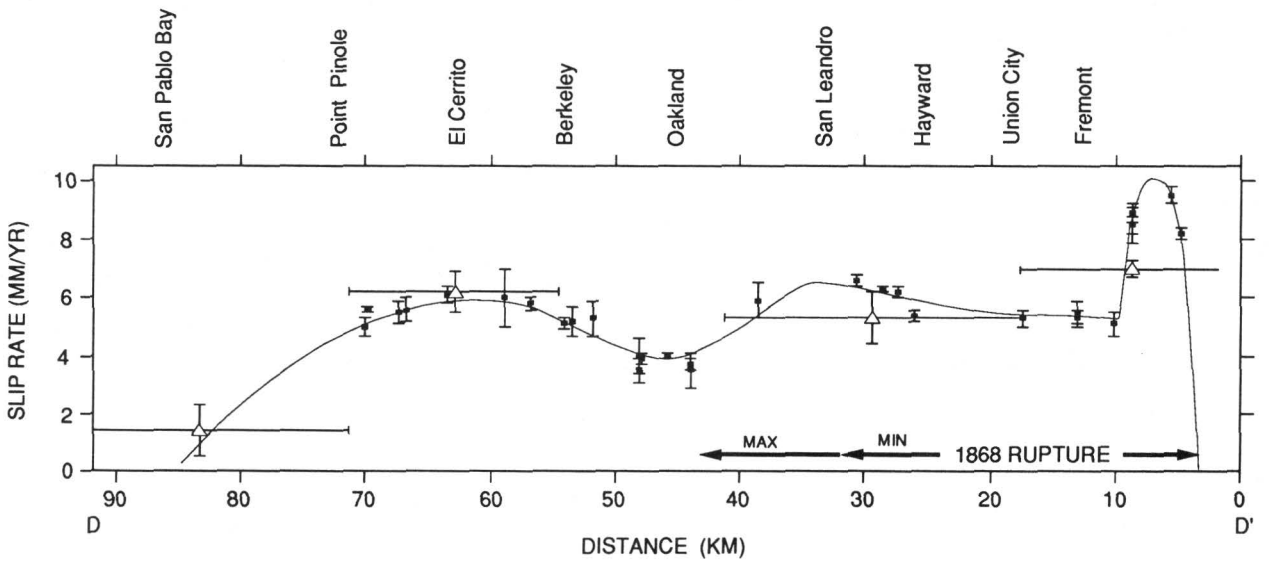

Figure 8. Slip rate along Hayward fault determined from offset cultural features and small-scale geodetic surveys (solid squares with ±1 standard deviation error bars). Curve represents polynomial fit to data. Also shown are slip rates (open triangles) corresponding to change of distance between geodetic monuments, with nearest benchmark located at a perpendicular distance of 2 to 4 km from fault trace. Horizontal bar indicates length of network projected onto section, open triangle marks center of line, and vertical bar shows ±1 standard deviation error. Horizontal arrows at bottom of figure show extent of 1868 rupture; "MAX" and "MIN" refer, respectively, to maximum and minimum estimates of northwest extent of rupture. Endpoints of plot, D-D′, are shown in figure 2. Figure after J.J. Lienkaemper and others (written commun., 1990).

creeping at a rate of 5 to 6 mm/yr. An exception is the southern 5 km, which has been creeping at 8 to $9\frac{1}{2}$ mm/yr and at times has had creep rates as fast as 10.2 ± 0.5 mm/yr. The creep rates are comparable to the new geologic estimates, and both the geologic and creep observations may represent the minimum total rate of slip for the Hayward fault. The increase of our estimated slip rate to 9 ± 2 mm/yr reflects these new observations and their associated uncertainties. The relation

between surface creep and crustal stress accumulation is not well understood for the Hayward fault. For the calculation of probabilities we have assumed that the fault is locked at depth and is accumulating stress at a rate appropriate to 9 ± 2 mm/yr.

Slip Per Event

No new information has been obtained on the amount of coseismic slip that occurs during large–magnitude Hayward fault earthquakes. In the 1988 report a slip per event of 1.4 ± 0.4 m was used for both segments, on the basis of an empirical relation between fault length and displacement. The current Working Group felt that the 1988 value suggested a degree of precision that was too high. For the present report the displacements for both segments have been revised to 1.5 ± 0.5 m. This value, and its uncertainty, are based on both the empirical relationship between length and displacement and the amount of slip often associated with earthquakes comparable to the historical earthquakes ($M \sim 7$) on these segments.

Recurrence Interval

The mean recurrence interval for each Hayward fault segment derived from the slip rate and slip per event values is 167 ± 67 years.

Probabilities

Based on the input parameters above, the 30–year probabilities for the southern East Bay segment and northern East Bay segment are 0.23 and 0.28, respectively (table 8).

RODGERS CREEK FAULT SEGMENT

The Rodgers Creek fault is a major segment of the Hayward fault zone (fig. 6). It extends from about San Pablo Bay to at least as far north as Santa Rosa. The Rodgers Creek fault has long been recognized as an active fault. It appears on the 1975 State of California map (Jennings, 1975) as a Holocene fault and has an Alquist–Priolo Special Studies Zone along it (Hart, 1988). The Rodgers Creek fault was not included in the 1988 Working Group report because of an absence of information on slip rate, recurrence interval, and slip per event. New paleoseismic data, along with preliminary geodetic observations and microseismic data (fig. 7), indicate that the Rodgers Creek fault zone has a rate of activity comparable to that estimated for the Hayward fault and has the capability of causing large earthquakes.

Slip Rate

Trenches excavated where the fault offsets alluvial fan deposits, 18 km north of San Pablo Bay, have exposed buried channels offset by the fault (Budding and others, 1989). These channels have been offset 5 to 7 m and yield a slip rate of 3.9 to 5.5 mm/yr for the past 1,270 years (D.P. Schwartz, unpub. data, 1990). This is a minimum rate because the offset channel deposits were dated with detrital charcoal and are therefore younger, by an unknown amount, than the radiocarbon age. Unpublished geodetic data can be interpreted as placing 6 to 10 mm/yr of slip on the Rodgers Creek fault (Lisowski, written commun., 1990). These data are consistent with the 9 ± 2 mm/yr slip rate employed for the Hayward fault, and we have adopted the same rate for the Rogers Creek fault segment.

Slip Per Event and Recurrence Interval

At present there is no information on the timing of past large earthquakes on the Rodgers Creek fault. Preliminary estimates of recurrence can be made using two methods. First, slip per event can be divided by slip rate. A gully and adjacent surface debris flow at the trench site were

Table 8. Probabilities of earthquakes along Hayward and Rodgers Creek faults

Segment	Previous event	Expected magnitude	Probability[1] 1990–2020	Level of reliability (scale of A to E; A most reliable)
Southern East Bay	1868	7	0.23	C
Northern East Bay	1836	7	.28	D
Rodgers Creek fault	1808 (or earlier)	7	.22	D

[1] Differences in probabilities of less than 0.10 are not considered meaningful.

offset 2.0 (+0.3, −0.2) m during the most recent event (Budding and others, 1989). Using this offset value with an uncertainty of ±0.5 m and the 9 mm/yr slip rate adopted for this segment yields an expected recurrence interval of 222 ± 74 years. Second, the number of events that occurred during the interval represented by the channel deposits can be used to calculate average recurrence. If the 2 m offset is a characteristic value, the 5 to 7 m represents 3 to 4 paleoearthquakes in a 1,270–year period. This gives a range of intervals from 254 to 635 years. These would be maximum values. For calculation of probabilities for this segment, we have used the 222 ± 74 year result.

Probabilities

It is uncertain how much time has elapsed since the most recent event capable of producing 2 m of surface offset. The 1898 Mare Island M 6½ earthquake is the largest historical event that could have occurred on the fault, but it appears to have been too small to produce the 2–m offset. Available descriptions of the Sonoma Mission do not indicate that it was damaged in 1836, although damage was reported from the 1868 Hayward event. An earthquake of 1808 caused damage in the Presidio in San Francisco. It is unknown what the source of this earthquake was, but the Rodgers Creek fault cannot be excluded. Therefore, the minimum elapsed time is set at 181 years. The 30–year probability (table 8) derived using this elapsed time and the previously discussed input parameters is 0.22. This should be considered a minimum value.

SUMMARY AND DISCUSSION

This report summarizes available information pertaining to large earthquakes in the San Francisco Bay region. By using the available information, reasonable assumptions, and simple models, it strives to make projections about the locations, sizes, and times of future earthquakes. The types of basic information used in this report include the following:

(1) Identification of fault segments judged to be capable of producing large earthquakes in the future.
(2) Estimates of the amount of displacement and thus the magnitude of future large earthquakes likely to occur during rupture of these fault segments.
(3) Estimates of the median recurrence intervals (and their uncertainties) for major earthquakes on the fault segments.
(4) Estimates of the date of the most recent large earthquake for each of the fault segments.

There is considerable uncertainty associated with each of these types of basic earthquake information. One of the principal tasks of the current Working Group was to examine and explore alternative explanations and interpretations of the data. The information about earthquakes in

the San Francisco Bay region will improve with better means of analysis and with additional data. The Working Group sees an urgent need for additional studies to reduce the uncertainty of the fault segment assessments considered in this report and to permit evaluation of other faults that may have the potential for producing major earthquakes. In particular, knowledge of the average time interval between segment–rupturing earthquakes, which might be learned from paleoseismic studies, might permit major revisions of the consensus forecasts presented here. Studies aimed at providing dates of large earthquakes on the Hayward fault prior to 1836 are essential.

In its present form, even with its inherent uncertainty, this basic information has something to say about future large earthquakes in the San Francisco Bay region. Several fault segments have a demonstrated capability of causing large earthquakes. Furthermore, for several of these segments the time interval that has elapsed since the last earthquake is approaching the estimated recurrence interval, which means that large earthquakes on these segments in the coming decades are not only possible, but likely.

The method of using this basic information to develop probabilistic assessments followed the general procedures employed in the previous Working Group report (1988). Results of the current study are summarized in figure 9.

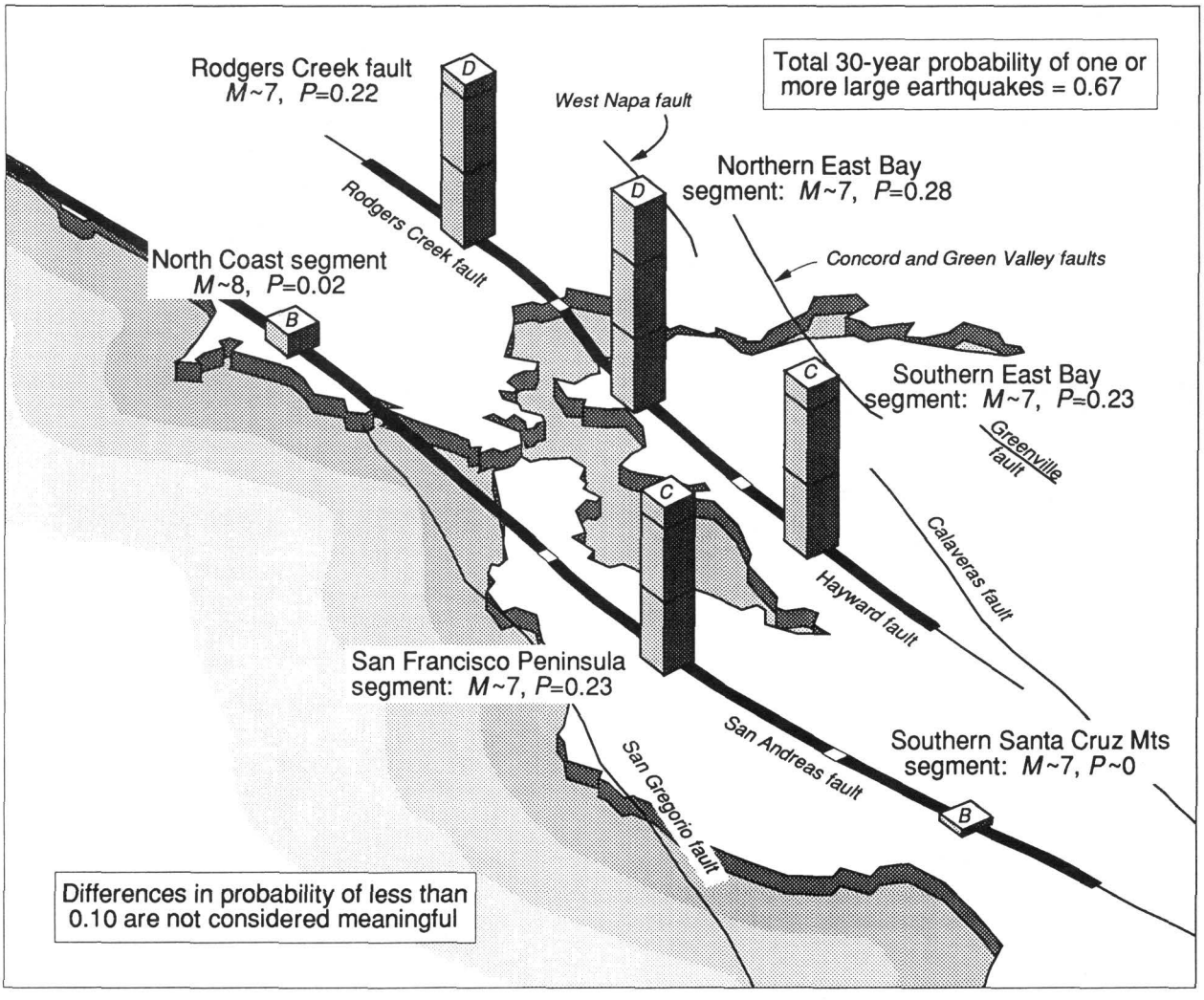

Figure 9. Conditional probabilities of earthquakes ($M \geq 7$) in San Francisco Bay region. Column heights are proportional to probabilities. Letters on columns indicate reliability of forecast, on a scale of A to E, with A being most reliable. M, magnitude; P, probability.

The principal revisions and additions to the previous report include the following:

(1) Segment boundaries were revised on the San Francisco Peninsula as a consequence of the Loma Prieta earthquake, and along the Hayward fault as a result of a review of geological, geophysical, and historical data.
(2) The preferred San Andreas fault slip rate was revised upward from 16 ± 2.5 mm/yr to 19 ± 4 mm/yr. This change shortens the expected earthquake recurrence times.
(3) The effects of stress changes on the time of earthquake recurrence caused by the Loma Prieta earthquake have been considered. The effect of the estimated stress changes is to decrease the recurrence time of the northern Santa Cruz Mountains segment possibly by as much as 25 to 30 years (table 4). This possible effect becomes less important with increasing distance from the Loma Prieta earthquake rupture.
(4) The slip rate on the Hayward fault was revised from 7.5 ± 2.0 mm/yr to 9.0 ± 2 mm/yr. This change also tends to reduce expected recurrence times.
(5) Information on earthquake recurrence and slip per event has become available for the Rodgers Creek fault, permitting an assessment of its potential for generating a major earthquake.

Although the potential for damage from an earthquake generally decreases as distance from the epicentral region increases, the pattern of losses at rather large distances from the M 7.1 Loma Prieta earthquake clearly demonstrates that an earthquake on any of the fault segments considered by the Working Group could seriously affect the entire San Francisco Bay region. Indeed, the most densely populated parts of the area lie atop of or adjacent to fault segments having the greatest potential for large earthquakes. Table 9 gives the combined probabilities of one or more large earthquakes in the San Francisco Bay region. These combined probabilities, referred to here as total or aggregate probabilities, are obtained from aggregating the probabilities of the individual segments following the procedure employed in the 1988 report. Total probabilities for 5–, 10–, 20–, and 30–year intervals beginning at the start of 1990 have been calculated. The aggregated probability, P, is obtained from

$$P = 1 - (1 - P_a)(1 - P_b)(1 - P_c)\cdots, \tag{11}$$

where P_a, P_b, and P_c are the individual probabilities for earthquakes on segments a, b, and c, respectively, for the interval of interest. Application of equation (11) assumes independence of the individual events, which is not strictly true given that segments share uncertain slip rates.

The revisions leading to the interpretation of higher slip rate on the San Andreas and Hayward faults and the calculations of increased fault stress due to the Loma Prieta earthquake all tend to decrease the expected recurrence times and thereby increase the probability of major earthquakes along the San Andreas and Hayward faults.

We now conclude that the total 30–year probability of one or more major earthquakes in the San Francisco Bay region is 0.67 (table 9). This represents a significant increase from the value of 0.5 of the previous Working Group report (1988). About half of this increase can be ascribed to the addition of the Rodgers Creek fault segment to the list of potential major earthquake sources. The remaining increase is due to the increases of earthquake probabilities on the individual fault segments described above. In the previous report the southern Santa Cruz Mountains segment was assigned a probability of 0.3, but that segment was not included in the 1988 aggregated probability.

As these numbers make clear, the estimated probability of a major earthquake in the San Francisco Bay region has increased from the 1988 report. In addition, we emphasize that the estimate of total probability may represent a minimum value. This is because other faults, for which there is insufficient information to presently conduct an analysis of this type, particularly the San Gregorio, Calaveras, Greenville, Concord, Green Valley, and West Napa faults, may have

Table 9. Probabilities of one or more large earthquakes in San Francisco Bay region

Segments	Probability for intervals beginning 1/1/90				Level of reliability (scale of A to E; A most reliable)
	5 yr	10 yr	20 yr	30 yr	
North Coast, San Francisco Peninsula, N. East Bay, S. East Bay, and Rodgers Creek	0.15	0.33	0.50	0.67	B

the potential for producing major earthquakes in the San Francisco Bay region. Indeed, of the likely 33–40 mm/yr displacement rate that is believed to occur across the entire San Andreas fault system, only 28 mm/yr is accounted for in the present assessment of the San Andreas fault proper and the Hayward and Rodgers Creek faults.

There is a consensus among all who have studied the large–scale motions across the San Andreas fault system at the latitude of San Francisco Bay that strain is currently accumulating and will be released in future large–magnitude earthquakes (Ellsworth and others, 1981; Prescott and Yu, 1986; Scholz, 1990). In view of this strong conclusion, the question of another earthquake reduces from "if" to "when" and "where." This report presents one approach to this problem. As a counterpart to this fault–specific approach, the aggregate probability of one or more M 7 earthquakes during the next 30 years can also be determined using a more traditional, time–independent method.

The rate of occurrence of earthquakes in a region may be modelled as a Poisson process in which the probability of one or more events in a time interval t is $P = 1 - e^{-\lambda t}$, where λ is the average rate of earthquake occurrence. Two estimates of λ for $M \geq 7$ earthquakes are available for the San Francisco Bay region. One is obtained by noting that four such events have occurred since the 1836 earthquake (in 1838, 1868, 1906, and 1989), giving $\lambda = 0.026$/year. Over a 30–year period, $P = 0.54$. The other estimate derives from the Gutenberg–Richter frequency–magnitude distribution of smaller earthquakes in the region. The annual frequency of $M \geq 7$ earthquakes has been estimated as $\lambda = 0.017$/year (Collins and others, 1989), leading to a 30–year estimate of $P = 0.40$. While each of these Poisson estimates is smaller than our preferred value of $P = 0.67$, they too suggest a serious possibility of damaging earthquakes in the coming decades.

In addition, three other lines of argument, based on earthquakes prior to 1906, suggest that the likelihood of large earthquakes in the San Francisco Bay region in the coming decades is as great as or possibly greater than the above probabilities indicate. The first is the seismic cycle argument. It has long been noted (Tocher, 1959) that seismic activity in the San Francisco Bay region was much higher during the 70 years preceding 1906 than in the 70 years following. On the basis of an increase in activity in the late 1970's, Ellsworth and others (1981) suggested that the quiet portion of the cycle was over and that M 6–7 earthquakes might be expected at the rate of one per decade or more; subsequent events suggest that their estimate was too low. If the analogy with the 19th century is correct, then the 30–year Poisson probability of $M \geq 7$ earthquakes (based on the earthquakes of 1836, 1838, 1868, and 1906) is estimated to be 0.72.

The second argument pertains to the pairing of large earthquakes in this region in the nineteenth century. In 1836, there was a M 7 event on the northern half of the Hayward fault, and two years later, a M 7 event on the San Francisco Peninsula. In 1865, there was a M 6.5 earthquake, possibly on the same segment of the San Andreas fault that produced the recent Loma Prieta earthquake, and it was followed three years later by a M 7 earthquake on the southern Hayward fault (Toppazada and others, 1981). Such pairing could be coincidence, of course, and we have no physical model that supports a causal connection. Conversely, we cannot confidently dismiss the pattern as coincidence.

The third argument is based on a comparison of earthquakes along the Calaveras faults since 1979 with the earthquakes in the decade preceding the 1868 Hayward earthquake. The 10 years prior to the 1868 Hayward earthquake were characterized by a high rate of activity primarily along the northern Calaveras fault, including six events between M 5.5 and M 6.1 (Ellsworth and others, 1981). Since 1979 there have been four events of M 5.5 to M 6.1 in the same general area, an area which had not had any events larger than M 5.5 since 1911. In addition, since 1979 there has been a clear progression of activity from south to north along the southern Calaveras fault; the most recent activity has been near Alum Rock, just south of the point where the Calaveras and Hayward fault systems intersect (Oppenheimer and others, 1990). If this propagation of activity continues to the northwest, it might well involve a transfer of stress to the Hayward fault, potentially raising the likelihood of a repeat of the 1868 Hayward event. It should also be noted that a sequence of M 5–6 earthquakes occurred on the same section of the Calaveras fault between 1897 and 1911. This was not followed by a large earthquake on the Hayward fault. However, the earthquake in 1897 and the two events in 1903 occurred at a time of heightened regional activity that culminated in the 1906 earthquake.

Finally, it is instructive to compare these revised results for the San Francisco Bay region with those of the 1988 report for other parts of California. The Parkfield segment of the San Andreas fault in central California, with an estimated 30–year probability of >0.9 for a moderate–size (M 6) earthquake, remains the segment with the highest probability of rupture in California, as well as one for which the level of reliability of the estimate is considered highest. In southern California, the highest 30–year probabilities for individual fault segments estimated in 1988 were 0.5 for the Imperial fault and 0.4 for the Coachella Valley segment of the San Andreas fault. For the entire southern San Andreas fault, the probability of one or more large earthquakes was estimated to be 0.6, and for the San Jacinto fault, 0.5; the probability would be still greater if the two faults were considered together. Many cities such as San Bernardino are close to both faults. Thus, these total probabilities are similar to the revised estimates for the San Francisco Bay region, although it should be emphasized that numerous active faults were not included in the evaluations for either area because of the lack of data. Furthermore, we again point out that a reevaluation of the 1988 estimates has not yet been carried out for southern California, where many new data have also been gathered recently, and the probability estimates could change there as in the San Francisco Bay region.

ACKNOWLEDGMENTS

The Working Group thanks the many individuals who cooperated in preparation of this report. We particularly wish to acknowledge the contributions of expertise and unpublished data from Karin Budding, Lynn Dietz, Timothy Hall, Brian Kilgore, James Lienkaemper, Michael Lisowski, Mark Matthews, David Oppenheimer, Carol Prentice, William Prescott, Paul Reasenberg, James Savage, and Robert Simpson. The National Earthquake Prediction Evaluation Council (chaired by Thomas McEvilly) and the California Earthquake Prediction Evaluation Council (chaired by James Davis) reviewed the report and offered numerous useful suggestions. William Bakun and Thomas Heaton provided additional detailed technical reviews. Helen Gibbons edited the report. The efforts of Nancy Arp in preparing this report and in arranging the meetings of the Working Group are especially appreciated.

REFERENCES

Addicott, W.A., 1969, Late Pliocene mollusks from San Francisco Peninsula, California, and their paleogeographic significance: Proceedings of California Academy of Sciences, Fourth Series, v. 37, p. 57–93.

Benjamin, J.R., and Cornell, C.A., 1970, Probability, statistics, and decision for civil engineers: New York, McGraw Hill, 684 p.

Budding, K.E., Schwartz, D.P., Ostergren, C.L., and Hoirup, D.F., 1989, Preliminary slip rate and earthquake recurrence on the Rodgers Creek fault zone, northern California [abs.]: Eos, Transactions of the American Geophysical Union, v. 70, p. 1211.

Chapman, R.H., and Bishop, C.C., 1988, Bouguer gravity map of California, Santa Rosa quadrangle: California Department of Conservation, Division of Mines and Geology, Regional Geologic Map Series, Map No. 2B, scale 1:250,000.

Collins, E.R., Chiou, S.-J., and Uhrhammer, R.A., 1989, Earthquakes and the registration of earthquakes from January 1, 1988 to December 31, 1988: Bulletin of the Seismographic Stations of the University of California, v. 58, nos. 1 and 2, p. 1–107.

Cummings, J.C., 1968, The Santa Clara Formation and possible post–Pliocene slip on the San Andreas fault in central California, *in* Dickinson, W.R., and Grantz, A., eds., Proceedings of conference on geologic problems of the San Andreas fault system, v. 11 *of* Stanford University Publications in the Geological Sciences: Stanford, Calif., School of Earth Sciences, Stanford University, p. 191–207.

Cummings, J.C., 1983, The Woodside Facies, Santa Clara Formation, and late Quaternary slip on the San Andreas fault, San Mateo County, California [abs.]: Program and abstracts for the 58th annual meeting, Pacific Sections, American Association of Petroleum Geologists, Society of Exploration Geophysicists, and Society of Economic Paleontologists and Mineralogists, Sacramento, Calif., May 18–21, 1983, p. 82.

Davis, P.M., Jackson, D.D., and Kagan, Y.Y., 1989, The longer it has been since the last earthquake, the longer the expected time till the next?: Seismological Society of America Bulletin, v. 79, p. 1439–1456.

Dieterich, J.H., 1988, Probability of earthquake recurrence with non–uniform stress rate and time–dependent failure: PAGEOPH, v. 126, p. 589–617.

Dietz, L.D., and Ellsworth, W.L., in press, The October 17, 1989 Loma Prieta, California, earthquake and its aftershocks: Geometry of the sequence from high–resolution locations: Geophysical Research Letters.

Ellsworth, W.L., in press, Earthquake history, 1769–1989, *in* Wallace, R.E., ed., The San Andreas fault system, California: U.S. Geological Survey Professional Paper 1515.

Ellsworth, W.L., Lindh, A.G., Prescott, W.H., and Herd, D.G., 1981, The 1906 San Francisco earthquake and the seismic cycle, *in* Simpson, D.W., and Richards, P.G., eds., Earthquake prediction, an international review: American Geophysical Union Maurice Ewing Monograph 4, p. 126–140.

Hagiwara, Y., 1974, Probability of earthquake occurrence as obtained from a Weibel distribution analysis of crustal strain: Tectonophysics, v. 23, p. 313–318.

Hall, N.T., 1984, Holocene history of the San Andreas fault between Crystal Springs Reservoir and San Andreas Dam, San Mateo County: Seismological Society of America Bulletin, v. 74, p. 281–299.

Hart, E.W., 1988, Fault-rupture hazard zones in California, Alquist-Priolo Special Studies Zones Act of 1972 with index to special studies zones maps [revised 1988]: California Division of Mines and Geology Special Publication 42, 24 p.

Hayford, J.F., and Baldwin, A.L., 1908, Geodetic measurements of earth movements, *in* Lawson, A.C., chairman, The California earthquake of April 18, 1906, Report of the State Earthquake Investigation Commission [reprinted 1969]: Carnegie Institution of Washington Publication 87, v. 1, p. 114–145.

Jennings, C.W., 1975, compiler, Fault map of California with locations of volcanoes, thermal springs, and thermal wells: California Division of Mines and Geology, Geologic Data Map, Map No. 1, scale 1:750,000.

Lawson, A.C., chairman, 1908, The California earthquake of April 18, 1906, Report of the State

Earthquake Investigation Commission [reprinted 1969]: Carnegie Institution of Washington Publication 87, 2 v. and atlas.

Lienkaemper, J.J., Borchardt, G., Wilmesher, J.F., and Meier, D., 1989, Holocene slip rate along the Hayward fault, northern California [abs.]: Eos, Transactions of the American Geophysical Union, v. 70, p. 1349.

Lindh, A.G., 1983, Preliminary assessment of long–term probabilities for large earthquakes along selected segments of the San Andreas fault system in California: U.S. Geological Survey Open–File Report 83–63, p. 1–15.

Lindh, A.G., 1988, Estimates of long–term probabilities for large earthquakes along selected fault segments of the San Andreas fault system in California, *in* Guha, S.K., and Patwardhan, A.M., eds., Earthquake prediction present status: Pune, India, University of Poona, p. 189–200.

Lindh, A.G., Moths, B.L., Ellsworth, W.L., and Olson, J.A., 1982, Historic seismicity of the San Juan Bautista, California, region, *in* Hill, D.P., and Nishimura, K., chairmen, Proceedings of the second joint meeting of the U.S.–Japan Conference on Natural Resources (UJNR) Panel on Earthquake Prediction Technology: U.S. Geological Survey Open–File Report 82–180, p. 45–50.

Lisowski, M., Prescott, W.H., Savage, J.C., and Johnston, M.J.S., in press, Geodetic estimate of coseismic slip during the 1989 Loma Prieta, California, earthquake: Geophysical Research Letters.

Louderback, G.D., 1947, Central California earthquake of the 1830's: Seismological Society of America Bulletin, v. 37, no. 1, p. 33–74.

Matsu'ura, M., Jackson, D.D., and Cheng, A., 1986, Dislocation model for aseismic crustal deformation at Hollister, California: Journal of Geophysical Research, v. 91, no. B12, p. 12,661–12,674.

Moths, B.L., Lindh, A.G., Ellsworth, W.L., and Fluty, L., 1981, Comparison between the seismicity of the San Juan Bautista and Parkfield regions, California [abs.]: Eos, Transactions of the American Geophysical Union, v. 62, p. 958.

Nason, R.D., 1971, Investigations of fault creep slippage in northern and central California: San Diego, Calif., University of California, Ph.D. dissertation, 231 p.

Nishenko, S.P., and Buland, R., 1987, A generic recurrence interval distribution for earthquake forecasting: Seismological Society of America Bulletin, v. 77, p. 1382–1399.

Nishenko, S.P., and Williams, P.L., 1985, Seismic hazard estimate for the San Jose–San Juan segment of the San Andreas fault: 1985–2005, *in* Shearer, C.F., ed., Minutes of the National Earthquake Prediction Evaluation Council, July 26–27, 1985, Menlo Park, California: U.S. Geological Survey Open–File Report 85–754, p. 351–366.

Olson, J.A., 1986, Seismicity of the San Andreas fault zone in the San Francisco Peninsula area, California: Bulletin of the Royal Society of New Zealand, v. 24, p. 87–97.

Oppenheimer, D.H., Bakun, W.H., and Lindh, A.G., 1990, Slip partitioning of the Calaveras fault, California, and prospects for future earthquakes: Journal of Geophysical Research, v. 95, no. B6, p. 8483–8498.

Plafker, G., and Galloway, J.P., 1989, Lessons learned from the Loma Prieta, California, earthquake of October 17, 1989: U.S. Geological Survey Circular 1045, 48 p.

Prentice, C.S., 1989, Earthquake geology of the northern San Andreas fault near Point Arena, California: Pasadena, Calif., California Institute of Technology, Ph.D. dissertation, 252 p.

Prescott, W.H., Lisowski, M., and Savage, J.C., 1981, Geodetic measurement of crustal deformation on the San Andreas, Hayward, and Calaveras faults near San Francisco, California: Journal of Geophysical Research, v. 86, p. 10,853–10,869.

Prescott, W.H., and Yu, S.–B., 1986, Geodetic measurement of horizontal deformation in the northern San Francisco Bay region, California: Journal of Geophysical Research, v. 91, no. B7, p. 7475–7484.

Reid, H.F., 1910, The mechanics of the earthquake, *in* Lawson, A.C., chairman, The California

earthquake of April 18, 1906, Report of the State Earthquake Investigation Commission [reprinted 1969]: Carnegie Institution of Washington Publication 87, v. 2, 192 p.

Rikitake, T., 1974, Probability of earthquake occurrence as estimated from crustal strain: Tectonophysics, v. 23, p. 299–312.

Sarna–Woycicki, A.M., Pampeyan, E.H., and Hall, N.T., 1975, Recent active breaks along the San Andreas fault between the central Santa Cruz Mountains and the southern Gabilan Range, California: U.S. Geological Survey Miscellaneous Field Studies Map MF–650, scale 1:24,000.

Savage, J.C., 1990, Criticism of some earthquake forecasts [abs.] (Seismological Society of America 85th annual meeting, Santa Cruz, Calif., May 1990): Seismological Research Letters, v. 61, no. 1, p. 43.

Savage, J.C., Prescott, W.H., Lisowski, M., and King, N., 1979, Geodolite measurements of deformation near Hollister, California, 1971–1978: Journal of Geophysical Research, v. 84, p. 7599–7615.

Scholz, C.H., 1985, The Black Mountain asperity: seismic hazard of the southern San Francisco peninsula, California: Geophysical Research Letters, v. 12, p. 717–719.

Scholz, C.H., 1990, The mechanics of earthquake faulting: Cambridge, Cambridge University Press, 439 p.

Schwartz, D.P., and Coppersmith, K.J., 1984, Fault behavior and characteristic earthquakes, examples from the Wasatch and San Andreas fault zones: Journal of Geophysical Research, v. 89, p. 5681–5698.

Shimazaki, K., and Nakata, T., 1980, Time–predictable recurrence model for large earthquakes: Geophysical Research Letters, v. 7, p. 279–282.

Sibson, R.H., 1984, Roughness at the base of the seismogenic zone: Contributing factors: Journal of Geophysical Research, v. 89, p. 5791–5800.

Sykes, L.R., and Nishenko, S.P., 1984, Probabilities of occurrence of large plate rupturing earthquakes for the San Andreas, San Jacinto, and Imperial faults, California: Journal of Geophysical Research, v. 89, p. 5905–5927.

Thatcher, W., 1975, Strain accumulation and release mechanism of the 1906 San Francisco earthquake: Journal of Geophysical Research, v. 80, p. 4862–4872.

Thatcher, W., 1979, Systematic inversion of geodetic data in central California: Journal of Geophysical Research, v. 84, p. 2283–2295.

Thatcher, W., and Lisowski, M., 1987, Long–term seismic potential of the San Andreas fault southeast of San Francisco: Journal of Geophysical Research, v. 92, p. 4771–4784.

Tocher, D., 1959, Seismic history of the San Francisco region, *in* Oakeshott, G.B., ed., San Francisco earthquakes of March 1957: California Division of Mines Special Report 57, p. 39–48.

Toppazada, T.R., Reel, C.R., and Parke, D.L., 1981, Preparation of isoseismal maps and summaries of reported effects for pre–1990 California earthquakes: California Division of Mines and Geology Open–File Report 81–11, 182 p.

Townley, S.D., and Allen, M.W., 1939, Descriptive catalog of earthquakes of the Pacific coast of the United States 1769 to 1928: Seismological Society of America Bulletin, v. 29, no. 1, p. 1–297.

Working Group on California Earthquake Probabilities, 1988, Probabilities of large earthquakes occurring in California on the San Andreas fault: U.S. Geological Survey Open–File Report 88–398, 62 p.

APPENDIX A–RECURRENCE MODELS

The earthquake probability estimates in this report are based on current stochastic recurrence models of characteristic earthquakes, including explicit consideration of the uncertainty in the values of the parameters of these models. By "characteristic earthquakes" we mean the relatively narrow range of large events associated with successive "complete" ruptures of a specific segment (for example, Schwartz and Coppersmith, 1984). The frequency of occurrence of such events is not necessarily predicted by extrapolation of the conventional (Gutenberg–Richter) linear (log) frequency–versus–magnitude relationship. Further, because characteristic earthquakes are associated with a "cycle" of major stress drop and stress recovery, it is believed that the inter–event, or recurrence, times of these events may follow a temporal pattern associated with a relatively narrow probability distribution (relative in this case to the exponential distribution associated with the reference case, a Poissonian recurrence model). In contrast to the Gutenberg–Richter magnitude–frequency distribution and the familiar Poisson recurrence model, the two general characteristics of this report's models, that is, a relatively narrow magnitude (or slip per event) range and a relatively narrow recurrence time distribution, are consistent with the notions of near–constant strain rate and a nearly deterministic characteristic earthquake cycle. Furthermore, in this mechanical context, these two characteristics are also consistent with each other. As long as some degree of proportionality exists between actual successive earthquake slips and recurrence times—for example, that proportionality associated with a constant slip rate[1]—this narrowness of one distribution will imply the narrowness of the other.

There are many probabilistic models that display these two basic characteristics. The discussion here is limited, first, to the simplest, the renewal model, because it has been widely studied, and second, to the time–predictable model favored by the current Working Group. The developments for the first are easily extended to the second. In both cases the recurrence time, T, follows a probability distribution, $f_T(t)$, with (marginal) median value, $\hat{T}$, and variability or dispersion measure, σ. In this report the dispersion measure is defined to be the standard deviation of the (natural) logarithm of T. In the range of our interest, this parameter is approximately equal to the coefficient of variation, that is, the standard deviation divided by the mean of the recurrence times. Various distribution types have been used in the literature for $f_T(t)$, including normal, lognormal, Weibull, and gamma. For any single segment there is insufficient data to distinguish among these distribution types; fortunately the majority of forecasts in this report are insensitive to the choice. The Working Group's general policy has been to retain the assumptions of the 1988 Working Group unless more recent evidence compels us to do otherwise. Therefore the lognormal distribution has been used again in this report. Research by Nishenko and Buland (1987) supports this assumption.

RENEWAL MODEL

The renewal model for characteristic events on a segment is based on the assumption of (probabilistic) independence among the sequence of recurrence times (T_1, T_2, ...) and the sequence of slips per event (D_1, D_2, ...). Probability forecasts are based on conditional probability statements, the condition being that no event has occurred between the previous event and the day of the forecast, that is, that a time, T_e, has elapsed since the last event. For the renewal model, the forecast for the next 30–year interval is written

[1] Note, however, that there is always proportionality between the *mean* (or median) of the slips per event and the *mean* (or median) of the recurrence times (by definition of the slip rate), even if, for example, the characteristic earthquakes occur in a Poisson fashion.

$$C_{30}^{T_e} = P[T_e < T \leq T_e + 30 \mid T \geq T_e]$$
$$= \frac{F_T(T_e + 30) - F_T(T_e)}{1 - F_T(T_e)}, \qquad (A-1)$$

in which the cumulative distribution function, $F_T(t)$, is related to the density function by

$$F_T(t) = P[T \leq t] = \int_o^t f_T(u)du. \qquad (A-2)$$

A graphical interpretation of equation (A–1) is given in figure A–1. Equation (A–1) is equivalent to equation 2 in the main body of the report. Typical plots of the function $C_{30}^{T_e}$ versus T_e (for given parameter values, $\hat{T}$ and σ) are shown in figure A–2. The value of σ dictates the sensitivity of the forecast to the elapsed time; for $\sigma \cong 1.0$, the probability is virtually independent of the elapsed time. (More precisely, for an exponential recurrence distribution, that is, for a Poissonian recurrence model, which has a coefficient of variation of 1.0, $C_{30}^{T_e}$ is independent of T_e. In other words, the Poisson process has no memory. Note that, in general, when T_e is about two–thirds of $\hat{T}$, the hazard is approximately equivalent to that of the Poisson model no matter what the value of σ. See fig. A–2.)

PARAMETRIC UNCERTAINTY

In practice it is difficult to know with precision the numerical values of parameters in this model for a specific fault. Following the practice of the 1988 Working Group (and practice in the engineering seismic hazard community), we treat the uncertain parameters in turn as random variables. The simplest model of parametric uncertainty considers only $\hat{T}$, the median, as uncertain and ignores the uncertainty in the dispersion measure. For reasons that will become clear below, this Working Group concurs with the 1988 Working Group in adopting this parametric uncertainty model and, further, in using a common value of 0.21 for the measure of variability of recurrence times. (The basis for this particular numerical value is the report by Nishenko and Buland (1987), who found it to be a representative value for circum–Pacific segments.) It will be seen below that the precise value of this parameter estimate is not critical provided it is less than about 0.3. Again like the 1988 Working Group, we assume that the parametric uncertainty in the median, $\hat{T}$, can be represented by a lognormal (prior) distribution with a specified best–estimate (median) value and a specified parametric uncertainty measure, denoted σ_P, which is the standard deviation of the (natural) log of the uncertain median. In this report, σ_P reflects the combined uncertainty in the slip per event and slip rate whose ratio is used to estimate the median $\hat{T}$. Typical values are about 0.4 (tables 3 and 7).

The simplest way to deal with parametric uncertainty is to "fold it in" with the intrinsic, obtaining what is called a "predictive distribution" on the recurrence T. For the assumptions here it can be shown (for example, Benjamin and Cornell, 1970, Chapter 6) that the predictive distribution of T is again lognormal with median $\hat{T}$ and net uncertainty parameter, σ_N:

$$\sigma_N = \sqrt{\sigma_P^2 + \sigma_I^2}, \qquad (A-3)$$

in which σ_I is now used to denote the "intrinsic," random, or event–to–event recurrence–time variability observed on a given segment, the parameter which was set equal to 0.21 in the discussion above. With this approach, one can again use equation (A–1) to calculate "the" conditional probability of an event in the next 30 years given an elapsed time interval of T_e years. The result is "the" value of this probability in that it has effectively considered each possible value of $\hat{T}$ and its relative likelihood (multiplied times the 30–year probability associated with that value of $\hat{T}$). As we shall see below, the result can also be interpreted as a *mean* estimate of this conditional probability,

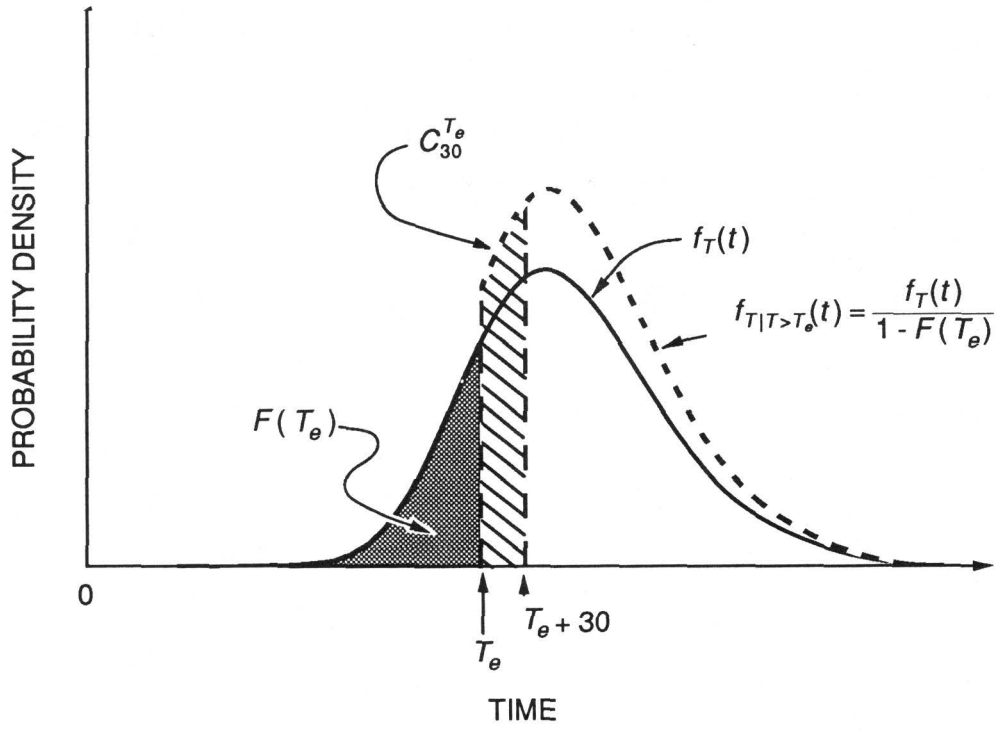

Figure A-1. Graphical interpretation of $C_{30}^{T_e}$, the conditional probability of $T_e \leq T \leq T_e + 30$ given $T > T_e$. See text for explanation of variables.

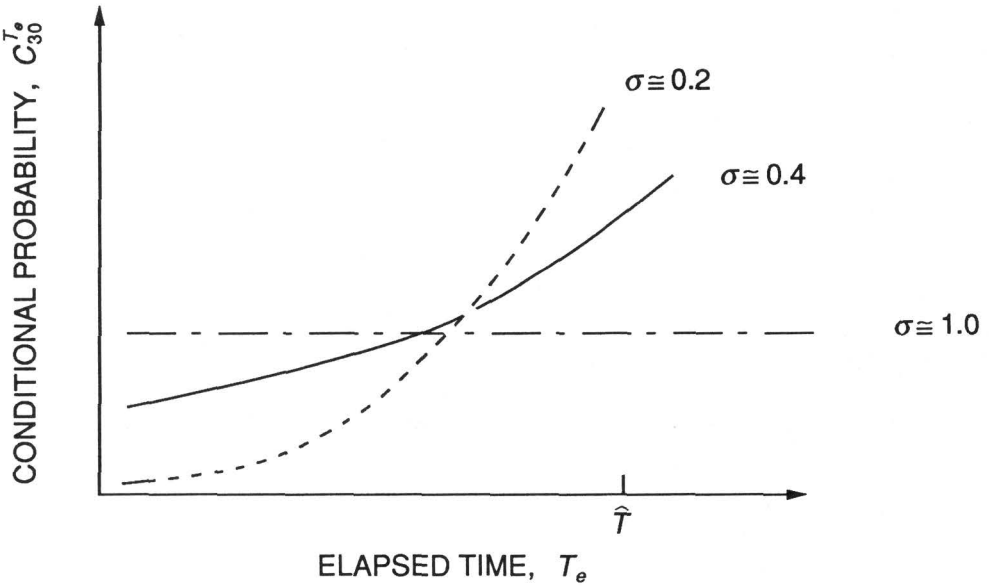

Figure A-2. Conditional probability, $C_{30}^{T_e}$, of an earthquake in the next 30 years given an elapsed time of T_e since the last event, for several values of σ, the degree of dispersion in the recurrence-time distribution. (Assumption: Recurrence interval, $\hat{T}$, is much greater than 30 years.)

$C_{30}^{T_e}$. Equation (A–3) explains why these estimates of $C_{30}^{T_e}$ are insensitive to the intrinsic variability σ_I: if the parametric uncertainty, σ_P, is approximately 0.4 or more, then the net uncertainty, σ_N, is insensitive to σ_I, provided σ_I is less than about 0.3.

It has been found effective when dealing with technical probability assessments to report more than simply a best estimate; we can also make explicit the degree of uncertainty in the estimates. Here the parametric uncertainty in the median (represented by the value of σ_P) induces uncertainty in $C_{30}^{T_e}$. If we rewrite equation (A–1) as

$$C_{30}^{T_e}(\hat{T}) = \frac{F_T(T_e + 30; \hat{T}) - F_T(T_e; \hat{T})}{1 - F_T(T_e; \hat{T})}, \qquad (A-4)$$

it emphasizes the fact that $C_{30}^{T_e}$ is a function of the uncertain parameter $\hat{T}$. (It is understood in this paragraph that the distribution $F_T(t; \hat{T})$ has for its dispersion level only the intrinsic value, σ_I, that is, 0.21 in these calculations.) Assuming that $C_{30}^{T_e}(\hat{T})$ is monotonically decreasing in $\hat{T}$ in the range of interest, we can find the fractile, c', of $C_{30}^{T_e}$ by calculating the probability that $\hat{T}$ is less than the corresponding value of the median, t'. (For a given value of c', the corresponding value of t' is found by solving equation (A–4) for $\hat{T}$.) To calculate this probability we must use the distribution on the uncertain parameter $\hat{T}$. This computation is complicated somewhat by the fact that the distribution on $\hat{T}$ must be "updated" to reflect the information that this particular, current recurrence time is greater than T_e, the elapsed time since the last event (see, for example, Davis and others, 1989). The updating uses Bayes theorum:

$$f''_{\hat{T}}(t \mid T > T_e) = k\, f'_{\hat{T}}(t)\, P[T > T_e \mid \hat{T} = t]. \qquad (A-5)$$

In this equation $f'_{\hat{T}}(t)$ is the "prior" distribution on the uncertain median (here lognormal with dispersion σ_P), while $f''_{\hat{T}}(t|T>T_e)$ is the "posterior" distribution (given the observation that $T > T_e$). Note that $f'_{\hat{T}}(t)$ is modified by the "likelihood function" (that is, the likelihood of the observation given that the true median, $\hat{T}$, has value t), which here is $P[T > T_e \mid \hat{T} = t]$. This probability is obtained from the (intrinsic; $\sigma = \sigma_I$) distribution on the recurrence time, T, but as a function of its median, $\hat{T}$. In this application $P[T>T_e|\hat{T}=t]$ varies from zero to one as t increases; for example, if the true median is very small, it is unlikely that one would have observed a recurrence interval as large as T_e. Therefore, such small values of $\hat{T}$ are "downweighted." Finally, the coefficient k in equation (A–4) is a normalizing factor that "ensures" that the posterior distribution on $\hat{T}$ has unit area. In practice these computations are conducted by numerical integration (or simulation). Making the calculations at a set of values, c', defines the probability distribution on the uncertain forecast $C_{30}^{T_e}$ induced by the uncertainty in the parameter $\hat{T}$. From this distribution one can read specified fractiles, for example, quantiles corresponding to probabilities of 0.25, 0.5, and 0.75. Results of such calculations appear in appendix C. In addition to fractiles, one can calculate the mean of the distribution of $C_{30}^{T_e}$; it can be shown that it is equivalent to "the" probability calculated from equation (A–1) using the predictive distribution on T, that is, using the total uncertainty σ_N (equation (A–3)). Therefore this result, which was also used by the 1988 Working Group, implicitly includes the updating of the distribution on the median due to the "open interval" information, $T > T_e$.

TIME–PREDICTABLE MODEL

In contrast to the renewal model, the time–predictable model of characteristic earthquake recurrence is based on the assumption that there is positive correlation between the slip, D_i, in a particular event on a segment and the subsequent recurrence time, T_i, to the next event. Further, some form of proportionality is assumed between the recurrence time and the slip. In this report

we adopt the probabilistic model

$$T_i = \frac{1}{V} D_i \epsilon_i \ , \qquad (A-6)$$

in which D_i is the (random) slip in the i^{th} characteristic earthquake in a sequence, T_i is the subsequent recurrence time to the next event, V is a constant (the constant slip rate), and ϵ_i is an (independent) random deviation term (with unit median value). Then, as discussed above, the (marginal) median of T is equal to the (marginal) median of D (that is, the median slip per event) divided by the slip rate, V. Conditional on knowing that the slip D_i was, say, d, the conditional median of T_i is d/V. Further, noting that $\ln T_i = -\ln V + \ln D_i + \ln \epsilon_i$, we see that σ, the marginal standard deviation of the log of T, is $\sqrt{\sigma_D^2 + \sigma_\epsilon^2}$, in which σ_D is the marginal (event–to–event) standard deviation of log D and σ_ϵ is the standard deviation of log E. In contrast, the conditional standard deviation of $\ln T$ (given D_i) is only σ_ϵ. (We retain the somewhat unusual notation of σ for standard deviation of the log of the variable.)

We need not repeat the results (equations (A–1) through (A–5)) for the time–predictable model. All the analysis developed above for the renewal model applies equally well to the time–predictable model, provided one interprets those distributions, parameters, and probabilities as *conditional* on the slip in the last event. For example, $\hat{T}$ and σ in equation (A–1) are now the conditional median and (log) standard deviation given the slip. The probability distribution functions F_T and f_T in equation (A–1) and (A–2) are those of the conditional distribution of T given D, and so on.

As stated, the Working Groups utilized the time–predictable model, and therefore the adoption of the lognormal type of distribution and the value $\sigma_t = 0.21$ are both strictly applicable to the *conditional* distribution on T given the past slip. For notational and editorial simplicity in the main body of the report, the notion that all is conditional on $D = d$ is normally deleted in the presentation. It is implicit. Note, as is clear in the model above, that the conditional (log) standard deviation of T is less than (or equal to) the marginal value. Hence, using 0.21 for the conditional value may be an upper bound because the Nishenko and Buland (1987) analysis, upon which the value is based, was conducted on marginal distributions. In fact there is as yet little evidence to establish the relative values of the marginal and conditional values of these dispersion measures, or equivalently the correlation coefficient[2] between $\ln D$ and the successive $\ln T$. Preliminary investigations show negligible estimated correlation between (estimated) characteristic *magnitudes* and logs of the succeeding recurrence times on a given segment, but the implied measurement noise (in relation to log *slips* and log times) is severe.

In the current application of these models to San Francisco Bay region forecasts there is little possibility to distinguish between the renewal and time–predictable model in any case. For virtually every segment there is only one past known earthquake. Therefore the best current estimate of the median slip per event, $\hat{D}$, is simply the slip in the last event, D. In this case the current estimate of the marginal median of T (that is, $\hat{D}/V$) is numerically equal to the conditional median of T given the past slip[3] (that is, D/V). The former is used in the renewal model and the latter in the time–predictable model. Provided one continues to use 0.21 for both the marginal and conditional variability measure, the two models will then produce the same forecast probability. As more information becomes available it will be possible to distinguish between the two.

---

[2] For the model in equation (A–6), the correlation coefficient between $\ln T$ and $\ln D$ is $\sigma_D^2/(\sigma_D^2 + \sigma_\epsilon^2)$, that is, σ_D^2/σ_T^2. The renewal model, incidentally, is obtained by replacing D_i by its median, $\hat{D}$, in equation (A–6).

[3] The slip in the last event, like the "constant" slip rate V, can only be estimated, of course, but that is a separate parameter–estimation problem discussed above and in the body of the report.

APPENDIX B–LOGIC-TREE ANALYSIS OF SAN ANDREAS FAULT PROBABILITIES

The Working Group has employed a logic tree to incorporate alternative interpretations of data and modeling of processes into the evaluation of earthquake probabilities. A logic–tree analysis consists of specifying the alternatives for potential outcomes or interpretations of parameters. Relative weights or likelihoods that a specific alternative is the correct one are assigned at branch points in the analysis (nodes). The sum of the branch weights at each node totals 1.00. For this study, the weights are based on the judgments of the Working Group and consist of the simple averages of weights polled from Working Group members.

Logic trees for earthquake probabilities on the southern Santa Cruz Mountains segment, the San Francisco Peninsula segment, and the North Coast segment are illustrated in figure B–1. Branch weights are indicated on the logic–tree diagrams. The logic–tree for the San Francisco Peninsula segment contains more branches than the others and serves as the basis for the following discussion.

SEGMENTATION

The first node of the San Francisco Peninsula segment logic tree arises from uncertainty over the segmentation of this part of the fault. The upper branch retains the single San Francisco Peninsula segment. The lower branch considers the possibility of earthquakes on two segments, the northern Santa Cruz Mountains segment and the mid–Peninsula segment. These alternatives are discussed in the report. We have assigned a likelihood of 0.56 to the single–segment branch and a likelihood of 0.44 to the two–segment branch.

RECURRENCE TIME

For each fault segment the next node represents the choice between models 1, 2, and 3 for estimating the median recurrence time, $\hat{T}$, and its associated parametric uncertainty, σ_P. The logic trees for the southern Santa Cruz Mountains and North Coast segments have only this single branching point. In each logic tree, the assigned weights for recurrence time models 1, 2, and 3 are 0.13, 0.47, and 0.40, respectively.

For models 1 and 2 the basis for the best estimate (the median) of $\hat{T}$ and its uncertainty measure, σ_P, are

$$\hat{T} = D/V,\ \sigma_P = \sqrt{\sigma_D^2 + \sigma_V^2}\ , \qquad (B-1)$$

where σ_P, σ_D, and σ_V are the standard deviations of the logs reflecting parametric uncertainty, respectively, of the uncertain median, $\hat{T}$, slip in the last event, D, and slip rate, V. The value of σ_D was estimated by the coefficient of variation of D, that is, by the standard deviation of the estimate, S_D, divided by the best estimate of D. The segment displacements, D, used in the model 2 calculations were estimated using a separate logic tree described later in this appendix.

For the case of model 3, $\hat{T}$ is based on $\hat{T}_{LP}$, the updated estimate of $\hat{T}$ for recurrence following the 1906 earthquake as given by equation (7) in the body of the report:

$$\hat{T}_{LP} = \exp\left\{\frac{\left[\frac{\log 132}{.31^2} + \frac{\log 83}{.21^2}\right]}{\left[\frac{1}{.31^2} + \frac{1}{.21^2}\right]}\right\},\ \sigma_P = \sqrt{\frac{1}{\frac{1}{.31^2} + \frac{1}{.21^2}}}\ . \qquad (B-2)$$

The estimate $\hat{T}_{LP}$ is equivalent to the weighted product (that is, a geometric mean):

$$\hat{T}_{LP} = 83^{W_1} 132^{W_2} = 83^{W_1} \left(\frac{D}{V}\right)^{W_2}, \qquad (B-3)$$

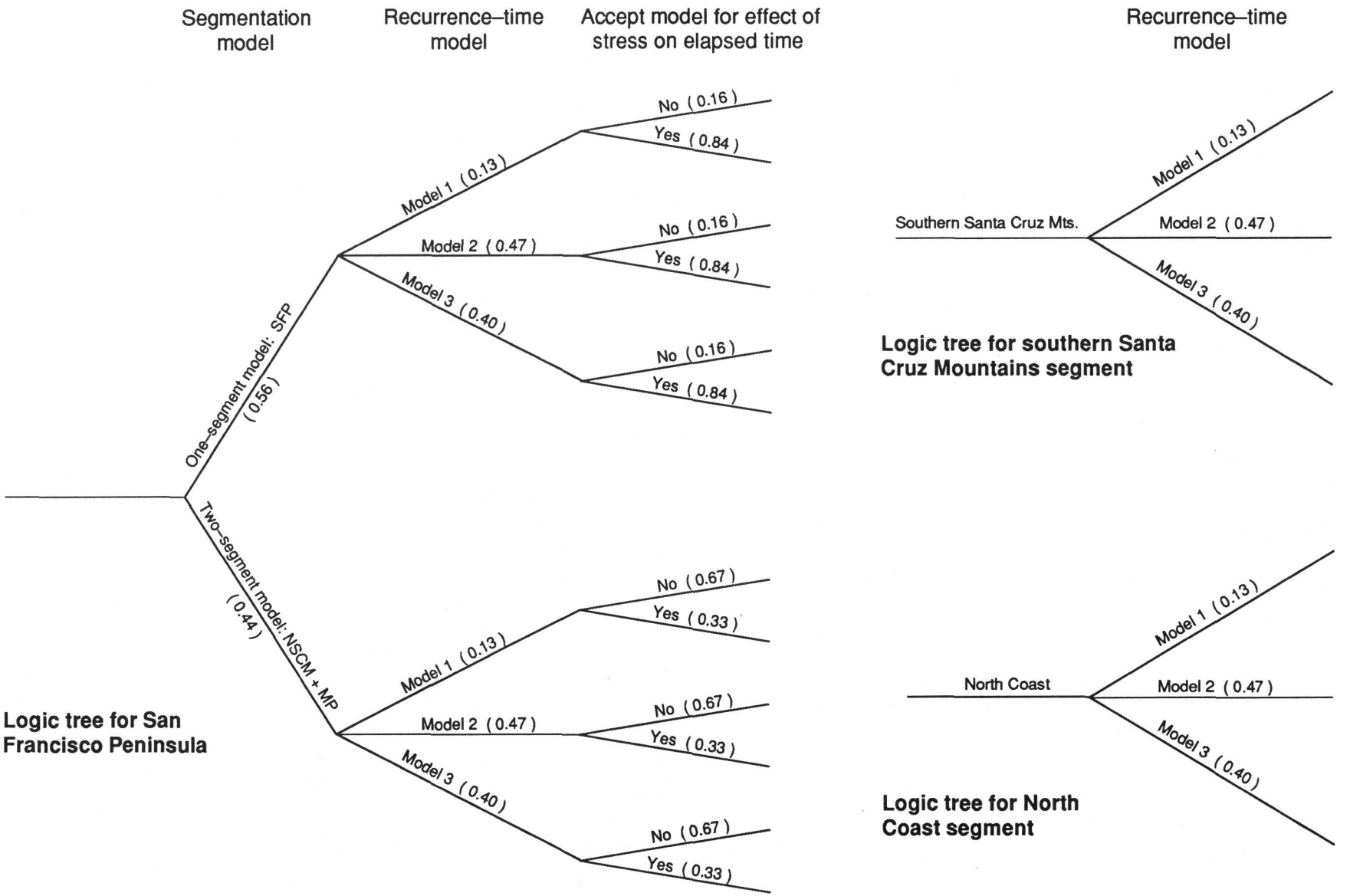

Figure B-1. Logic trees for San Francisco Peninsula, southern Santa Cruz Mountains, and North Coast segments of San Andreas fault. SFP, NSCM, and MP indicate branches for San Francisco Peninsula, northern Santa Cruz Mountains, and mid–Peninsula segments, respectively. Quantities in parentheses give assigned weight for the hypothesis represented by the branch.

in which

$$W_1 = 1 - W_2, W_2 = \left(\frac{\frac{1}{.31^2}}{\frac{1}{.31^2} + \frac{1}{.21^2}} \right). \qquad (B-4)$$

Hence, from the definition of recurrence–time model 3 (equation (6) in the report), the estimated recurrence time is

$$\hat{T} = 83^{W_1} \left(\frac{D}{V} \right)^{W_2} + \frac{\Delta D}{V}, \qquad (B-5)$$

where D is the estimated 1906 slip at Loma Prieta (2.5 ± 0.6 m), and ΔD is the difference between the 1906 slip on the segment of interest and the 1906 slip on the southern Santa Cruz Mountains segment. The approximate squared standard deviation of $\log \hat{T}$ can be found by first–order expansion (Benjamin and Cornell, 1970, p. 180):

$$\begin{aligned} \sigma_P^2 \cong \frac{1}{\hat{T}^2} \left\{ \left[83^{W_1} V^{-W_2} W_2 D^{W_2 - 1} \right]^2 S_D + V^{-2} S_{\Delta D}^2 \right\} \\ + \frac{1}{\hat{T}^2} \left\{ \left[83^{W_1} (W_{2-1}) D^{W_2} V^{-W_2 - 1} - \Delta D V^{-2} \right]^2 S_V^2 \right\}, \end{aligned} \qquad (B-6)$$

in which the S's are the standard deviations of the estimates of the indicated parameters.

EFFECT OF LOMA PRIETA STRESS CHANGES

The final node for the San Francisco Peninsula segment represents the decision of whether to accept or reject the calculations based on stress changes resulting from the Loma Prieta earthquake that reduce the expected recurrence time by an amount ΔT. The magnitude of ΔT is based on three–dimensional elastic dislocation calculations of the Loma Prieta earthquake slip that give the change of shear stress averaged over the entire segment of interest (R.W. Simpson and J.H. Dieterich, written commun., 1990). The branches for this node were independently weighted for the side of the tree having a single segment and for the side of the tree consisting of the two subsegments. For the single San Francisco Peninsula segment, a weight of 0.84 was assigned to branches that use the stress calculation to modify the expected recurrence times, and a weight of 0.16 was given to the branches that use the unmodified recurrence times. For the two–segment side of the tree, which considers the northern Santa Cruz Mountains segment and the mid–Peninsula segment, a weight of 0.33 was given to the branches that use the stress calculation to modify the expected recurrence times, and a weight of 0.67 was given to the branches that use the recurrence times unmodified by the calculated stress.

Details of the stress field in the zone of concentrated stresses near the edge of the Loma Prieta rupture surface are sensitive to model assumptions. Consequently, the effect of Loma Prieta stress changes is greatest but possibly most uncertain for the northern Santa Cruz Mountains segment, which is relatively small and is adjacent to the Loma Prieta rupture. The low weight assigned to the stress calculation in the two–segment branch reflects this uncertainty.

The best estimates of the median recurrence interval from models 1 and 2 and including the effect of Loma Prieta stresses are

$$\hat{T} = \frac{D - D'}{V}, \sigma_P = \sqrt{\sigma_{D-D'}^2 + \sigma_V^2}, \qquad (B-7)$$

where D' is the equivalent displacement reduction resulting from the stress effect given previously in table 4. For branches in which recurrence time is calculated using recurrence time model 3 and

including Loma Prieta stresses,

$$\hat{T} = 83^{W_1}\left(\frac{D}{V}\right)^{W_2} + \frac{\Delta D - D'}{V} . \qquad (B-8)$$

As in the case of equation (B–6), the approximate squared standard deviation of $\log\hat{T}$ can be found by first–order expansion. The result is the same as in (B–6) except that $(S^2_{\Delta D} + S^2_{D'})$ is used in place of $S^2_{\Delta D}$ and $(\Delta D - D')$ is used for ΔD.

HYPOTHESIS TESTS

It is our intention that as future large earthquakes occur (or do not occur) on the San Andreas and Hayward faults in northern California, our estimated recurrence times will form a quantitatively testable set of hypotheses. Such a test was performed above (see equation 4, in the body of the report) to test whether the time of occurrence of the Loma Prieta earthquake was consistent with the projections of the previous Working Group (1988).

To facilitate tests of our hypotheses in the future, we have attempted to state all relevant parameters relating to segmentation and recurrence time quantitatively and to place reasonable uncertainties on those parameters. However, because of the logic–tree analysis we have used for the San Andreas fault segments, precisely how to test recurrence–time hypotheses against future earthquakes may not be obvious. Hence, for each San Andreas fault segment we have computed a single median recurrence–time estimate, $\hat{T}$, and a net standard deviation, σ_N, to summarize our results in a simple way and in a form that is amenable to simple hypothesis tests (table B–1). The approximate median recurrence time for each segment that is given in table B–1 has been obtained by taking the weighted mean of the individual hypothesis $\hat{T}$ estimates listed in table 3:

$$\hat{T} = \sum W_i \hat{T}_i , \qquad (B-9)$$

where $\hat{T}_i$ is the recurrence time for hypothesis i. The net uncertainty, σ_N, given in table B–1 is computed for each segment by use of the following approximate formula:

$$S^2_N = \sum W_i(\hat{T}_i - \hat{T})^2 + \sum W_i S^2_{N_i} , \qquad (B-10)$$

where S_{N_i} and S_N are the standard deviations of the median recurrence time for hypothesis i and the weighted mean of the recurrence time for all hypotheses, respectively. Then the net standard deviation of the log of the median, σ_N, is given by

$$\sigma^2_N = \ln\left[(S^2_N/\hat{T}^2) + 1\right]. \qquad (B-11)$$

Although the recurrence parameters obtained from equations B–9, B–10, and B–11 and listed in table B–1 could be used to compute probabilities, those probabilities will differ slightly from the probabilities given in this report (the difference is 0.01 or less). This is because the reported probabilities are based on the weighted mean of the probabilities computed from the individual hypothesis parameters.

LOGIC TREE FOR MODEL 2 DISPLACEMENTS

Recurrence times for model 2 are dependent on the displacement, D, assigned to each segment. As discussed in the report, the amount of displacement that best characterizes the behavior of each segment has been one of the most difficult parameters to constrain. This is a result of differences between the 1906 geologic and geodetic observations and the lack of slip data from the 1838 and 1865 earthquakes. To ensure that all possible interpretations were accounted for, displacement logic trees were constructed for the three possible San Andreas fault segments (San Francisco

Table B–1. Weighted means of recurrence time, $\hat{T}$, and net uncertainty, σ_N, of San Andreas fault segments

Segment	Previous event	Expected magnitude	$\hat{T}$	σ_N
S. Santa Cruz Mountains	1989	7	90.9	0.31
N. Santa Cruz Mountains	1906	6.5	94.9	.51
Mid–Peninsula	1906	7	147.2	.40
San Francisco Peninsula	1906	7	136.3	.35
North Coast	1906	8	228.3	.36

Peninsula, northern Santa Cruz Mountains, and mid–Peninsula) (table B–2). The displacement alternatives contained in each logic tree represent values for which there was an observational basis or which could be derived from a segment length/displacement relationship or could be based on other geologic arguments. The length/displacement relationship employed here is $D = 2.8 \times 10^{-5} L$ (Working Group, 1988). Segment displacements and weights are given in table B–2.

The northern Santa Cruz Mountains segment contains five branches. Values are 0.6 m, a direct calculation using the rupture length of 22 km and the length/displacement relationship; 1.0 m, the maximum observed 1906 surface offset; 1.4 m, the 1906 Wright–Laurel tunnel offset, which, even though located just south of this segment, had a displacement similar to the 1989 displacement and might be representative of displacements for this part of the fault; 2.6 m, the average 1906 geodetic slip; and 3.3 m, the maximum allowable 1906 geodetic offset.

The mid–Peninsula segment has three branches. Displacement values are 1.1 m, the calculated value using a 40–km length and the length/displacement relationship; 2.5 m, the maximum measured 1906 surface offset; and 3.4 m, the maximum 1906 geodetic offset.

The single San Francisco Peninsula segment contains four branches. Displacement values are 1.8 m, a direct calculation using a 60–km rupture length and the length/displacement relationship; 2.5 m, the maximum 1906 surface offset; 3.0, an average of 1906 geologic and geodetic observations; and 3.5 m, the maximum 1906 geodetic offset.

PROBABILITIES

The final consensus probability of an earthquake on a segment is based on the weighted probability of each tip of the logic tree for that segment. The probability of an earthquake is found using the parameters ($\hat{T}, \sigma$, and T_e) appropriate to the branches leading to that tip. Probabilities for each segment tip are summarized in appendix C. The final probability of a segment–rupturing earthquake is the sum of the weighted probabilities. The weighting factor for a tip is the product of the branch weights leading to that tip. For a given segment the sum of the weights equals 1.00.

For the San Francisco Peninsula segment, where two segmentation alternatives have been considered, segment probabilities are subject to additional weighting by the segmentation weights. For example, the 30–year probability of an earthquake affecting the entire San Francisco Peninsula segment is the segment probability of 0.25 multiplied by the weighting factor for that segmentation alternative (0.56) giving a probability of 0.14. Similarly, the 30–year probability of the alternate case, that of earthquakes affecting only the northern Santa Cruz Mountains and mid–Peninsula segments are $0.44 \times 0.41 = 0.18$ and $0.44 \times 0.20 = 0.09$, respectively. The expected magnitude of an earthquake on the northern Santa Cruz Mountains segment is about 6.5 compared to an expected magnitude of about 7.0 for both the San Francisco Peninsula and mid–Peninsula segments. Consequently, the total probability of an earthquake of about 7.0 originating on either the entire segment or the longer subsegment is $0.14 + 0.09 = 0.23$.

Table B–2. Displacement weights for recurrence time model 2

Displacement (m)	Weight	Weighted displacement
Northern Santa Cruz Mountains segment		
0.6	0.06	0.04
1.0	.15	.15
1.4	.36	.50
2.6	.42	1.09
3.3	.01	.03
		Final D=1.80*
Mid–Peninsula segment		
1.1	.20	.20
2.5	.54	1.35
3.4	.26	.88
		Final D=2.46*
San Francisco Peninsula segment		
1.8	.21	.38
2.5	.37	.93
3.0	.32	.96
3.5	.10	.35
		Final D=2.62

*Weighted displacements do not add up to the final displacement because of rounding error.

APPENDIX C–TABULATIONS OF PROBABILITIES

This appendix presents tabulated results of probability calculations for intervals of 5, 10, 20, and 30 years. Although the Working Group regards these probabilities to be significant only to the nearest tenth, we report the probabilities to two decimal places to permit quantitative comparison of our results with other calculations.

San Andreas fault segment probabilities for each of the logic–tree branches described in appendix B are shown in table C–1. The "final" segment probabilities are the weighted sums of the branch probabilities.

The final segment probabilities for the San Andreas, Hayward, and Rodgers Creek faults are listed in table C–2.

DISCUSSION OF UNCERTAINTIES

Throughout this report the Working Group has acknowledged the uncertainties in both the data and the models upon which our calculations are based. The procedure for calculating the values

Table C–1. Probabilities of logic-tree branch tips

[$\hat{T}$, recurrence time; σ_P, parametric uncertainty; M, magnitude; n.a., not applicable]

Model	Accept stress effect	$\hat{T}$ (years)	σ_P	Weight	Probability for intervals beginning 1/1/90 5 yr	10 yr	20 yr	30 yr
Southern Santa Cruz Mountains segment, M~7 (previous event=1989)								
1	n.a.	100±24	0.24	0.13	0.00	0.00	0.00	0.00
2	n.a.	84±24	.28	.47	.00	.00	.00	.00
3	n.a.	96±16	.17	.40	.00	.00	.00	.00
Northern Santa Cruz Mountains segment, M~6.5 (previous event=1906)								
1	no	156±45	.28	.09	.02	.04	.09	.15
1	yes	127±45	.34	.04	.04	.09	.19	.29
2	no	95±44	.44	.31	.08	.15	.29	.41
2	yes	70±43	.56	.16	.10	.18	.33	.45
3	no	96±36	.37	.27	.09	.17	.32	.45
3	yes	71±43	.56	.13	.10	.18	.33	.45
Mid–Peninsula segment, M~7 (previous event=1906)								
1	no	213±60	.27	.09	.00	.01	.02	.03
1	yes	210±60	.27	.04	.00	.01	.02	.04
2	no	129±49	.37	.31	.04	.09	.18	.27
2	yes	127±49	.38	.16	.04	.09	.18	.28
3	no	149±31	.21	.27	.02	.03	.09	.16
3	yes	147±30	.20	.13	.02	.04	.09	.17
San Francisco Peninsula segment, M~7 (previous event=1906)								
1	no	188±54	.28	.02	.01	.01	.04	.07
1	yes	176±53	.29	.11	.01	.02	.05	.10
2	no	138±40	.28	.08	.03	.06	.14	.23
2	yes	128±38	.29	.39	.04	.09	.18	.29
3	no	138±29	.21	.06	.02	.05	.13	.22
3	yes	129±28	.21	.34	.03	.07	.17	.29
North Coast segment, M~8 (previous event=1906)								
1	n.a.	281±76	.27	.13	.00	.00	.00	.00
2	n.a.	237±73	.30	.47	.00	.00	.01	.02
3	n.a.	201±49	.24	.40	.00	.00	.02	.03

Table C–2. Final probabilities
[M, magnitude. See text for explanation of $P_{1/4}$ and $P_{3/4}$]

Segment	Interval beginning 1/1/90 (years)	Conditional probability (mean)	Quartile probabilities $P_{3/4}$	$P_{1/4}$
S. Santa Cruz Mountains	5	0.00	0.00	0.00
M~7	10	.00	.00	.00
	20	.00	.00	.00
	30	.00	.00	.00
N. Santa Cruz Mountains[1]	5	.03	.05	.00
M~6.5	10	.07	.11	.00
	20	.13	.22	.02
	30	.18	.31	.04
San Francisco Peninsula[2]	5	.03	.03	.00
M~7	10	.06	.08	.00
	20	.14	.21	.01
	30	.23	.38	.02
North Coast	5	.00	.00	.00
M~8	10	.00	.00	.00
	20	.01	.00	.00
	30	.02	.01	.00
S. East Bay	5	.04	.05	.00
M~7	10	.08	.12	.00
	20	.16	.25	.01
	30	.23	.40	.02
N. East Bay	5	.05	.08	.01
M~7	10	.10	.16	.01
	20	.19	.32	.03
	30	.28	.46	.06
Rodgers Creek	5	.04	.05	.00
M~7	10	.07	.11	.01
	20	.14	.23	.02
	30	.22	.35	.04

[1] Subsegment of the San Francisco Peninsula segment. Probability includes segmentation weight.
[2] Weighted average of San Francisco Peninsula segment and mid–Peninsula subsegment probabilities.

of probability takes into account the quantifiable aspects of these uncertainties. The Working Group believes that the presentation of the estimates of probability is consistent with current practice in decision theory. The conditional probability obtained using the net uncertainty, σ_N, and reported here corresponds to the mean of the probabilities one would obtain from a sufficiently large number of calculations using only the intrinsic uncertainty, σ_I, and values of $\hat{T}$ repeatedly drawn from the posterior distribution on the uncertain median given that $T > T_e$ (see appendix A, equation A–5). Hence, we emphasize that the conditional probability obtained using σ_N represents "the" probability because it has considered all possible values of $\hat{T}$ and their relative likelihoods.

There is, however, a view as set forth by Savage (1990, and written commun., 1990) that a better presentation of the results of the calculations is to give the distribution of probabilities obtained from σ_I using values of $\hat{T}$ drawn from the distribution on the uncertain median. Thus, in addition to the mean probabilities, we report probabilities obtained using values of $\hat{T}$ at the first and third quartiles of the parametric distribution[1] and calculated with σ_I alone. These quartile

[1] The parametric distribution of $\hat{T}$ needs to be updated to reflect the information (equation 2) that $T > T_e$. See appendix A.

probabilities provide a measure of the range of probabilities permitted by the parametric uncertainty assuming fixed $\sigma_I = 0.21$. The probability at the first quartile, $P_{1/4}$, is the probability obtained using the value of $\hat{T}$ that is larger than 75 percent of the recurrence times in the distribution. Hence, there is a 25–percent likelihood that the actual probability (that is, the probability that would be obtained if $\hat{T}$ were perfectly known) is less than $P_{1/4}$ or a 75–percent likelihood that it is greater. Similarly, the probability of the third quartile, $P_{3/4}$, uses a value of $\hat{T}$ that is greater than 25 percent of the recurrence times in the distribution, and there is a 75–percent likelihood that the actual probability is less than $P_{3/4}$. There is a 50–percent chance that the actual probability lies between $P_{1/4}$ and $P_{3/4}$. For the San Andreas fault segments the quartiles were found by numerical integration of the weighted sum of the posterior parametric distributions (given $T > T_e$) employed in the logic–tree analysis.

Unlike other computations in this report, these quartile probabilities are quite sensitive to the detailed model and specific parameter values adopted. In particular, it can be shown that the calculated quartiles are very sensitive to the *ratio* of the intrinsic uncertainty, σ_I, to the parametric uncertainty, σ_P. In contrast, for a fixed net uncertainty, $\sigma_N = \sqrt{\sigma_I^2 + \sigma_P^2}$, and given $\hat{T}$, the mean probability will remain unchanged. Because of limited data for estimation of σ_I, particularly from strike–slip faults, the numerical value of σ_I may be rather uncertain. In addition, Savage (1990, and written commun., 1990) argues that σ_I may be different for different fault segments. Consequently, we believe the quartiles or other measures of the distributions of probabilities may not be well defined. However, because the net uncertainty is rather insensitive to σ_I, the mean probability is not very sensitive to σ_I. Figure C–1 uses the northern East Bay segment as an example to illustrate these effects. Savage argues that a large spread in the distribution of probabilities (for example, a large difference between $P_{3/4}$ and $P_{1/4}$) indicates low reliability of the assigned (mean) probability. However, note in figure C–1 that the distribution becomes *broader* as the uncertainty *decreases*. In keeping with the Working Group's general position, which is not to rely on results that are specifically dependent on details of a particular model, we recommend that these quartile values be used only with caution. The qualitative letter grades (for example, tables 5, 8, and 9) and statements regarding first–digit accuracy represent the Working Group's preferred position with respect to uncertainties in the segment and aggregated probabilities.

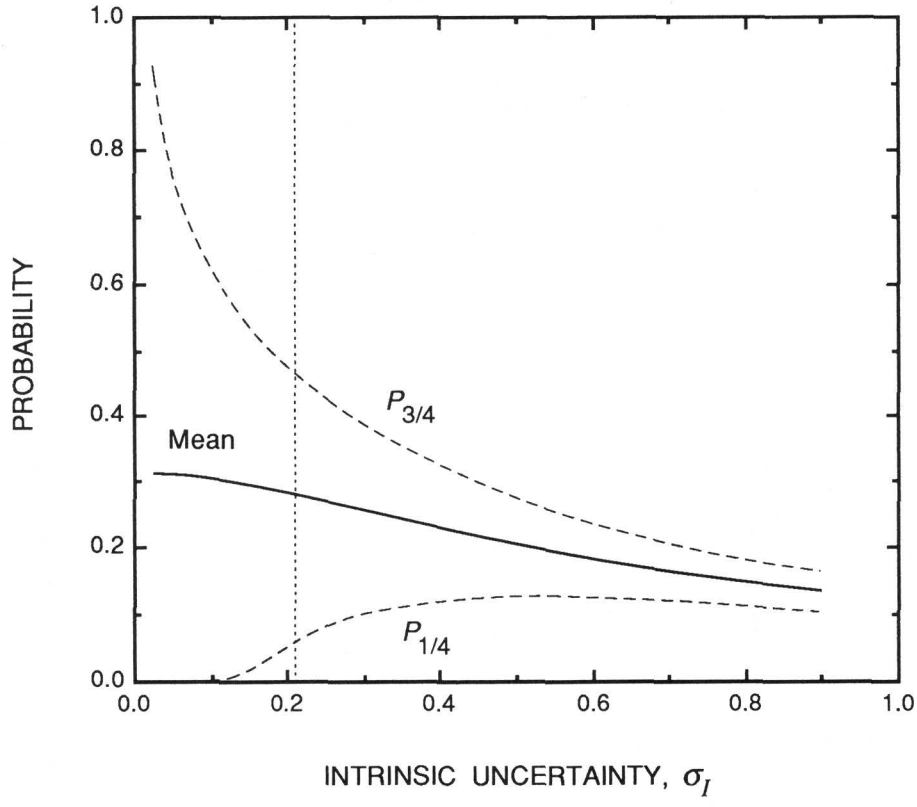

Figure C-1. Sensitivity of quartile probabilities ($P_{1/4}$ and $P_{3/4}$) and conditional probability (mean) to intrinsic uncertainty, σ_I. Dotted vertical line indicates value of σ_I (0.21) used in this study. Other parameters (median recurrence time, elapsed time, and parametric uncertainty) are fixed and are set equal to parameters used for northern East Bay segment. Time interval is 30 years.

SELECTED SERIES OF U.S. GEOLOGICAL SURVEY PUBLICATIONS

Periodicals

Earthquakes & Volcanoes (issued bimonthly).
Preliminary Determination of Epicenters (issued monthly).

Technical Books and Reports

Professional Papers are mainly comprehensive scientific reports of wide and lasting interest and importance to professional scientists and engineers. Included are reports on the results of resource studies and of topographic, hydrologic, and geologic investigations. They also include collections of related papers addressing different aspects of a single scientific topic.

Bulletins contain significant data and interpretations that are of lasting scientific interest but are generally more limited in scope or geographic coverage than Professional Papers. They include the results of resource studies and of geologic and topographic investigations; as well as collections of short papers related to a specific topic.

Water-Supply Papers are comprehensive reports that present significant interpretive results of hydrologic investigations of wide interest to professional geologists, hydrologists, and engineers. The series covers investigations in all phases of hydrology, including hydrogeology, availability of water, quality of water, and use of water.

Circulars present administrative information or important scientific information of wide popular interest in a format designed for distribution at no cost to the public. Information is usually of short-term interest.

Water-Resources Investigations Reports are papers of an interpretive nature made available to the public outside the formal USGS publications series. Copies are reproduced on request unlike formal USGS publications, and they are also available for public inspection at depositories indicated in USGS catalogs.

Open-File Reports include unpublished manuscript reports, maps, and other material that are made available for public consultation at depositories. They are a nonpermanent form of publication that may be cited in other publications as sources of information.

Maps

Geologic Quadrangle Maps are multicolor geologic maps on topographic bases in 7 1/2- or 15-minute quadrangle formats (scales mainly 1:24,000 or 1:62,500) showing bedrock, surficial, or engineering geology. Maps generally include brief texts; some maps include structure and columnar sections only.

Geophysical Investigations Maps are on topographic or planimetric bases at various scales; they show results of surveys using geophysical techniques, such as gravity, magnetic, seismic, or radioactivity, which reflect subsurface structures that are of economic or geologic significance. Many maps include correlations with the geology.

Miscellaneous Investigations Series Maps are on planimetric or topographic bases of regular and irregular areas at various scales; they present a wide variety of format and subject matter. The series also includes 7 1/2-minute quadrangle photogeologic maps on planimetric bases which show geology as interpreted from aerial photographs. Series also includes maps of Mars and the Moon.

Coal Investigations Maps are geologic maps on topographic or planimetric bases at various scales showing bedrock or surficial geology, stratigraphy, and structural relations in certain coal-resource areas.

Oil and Gas Investigations Charts show stratigraphic information for certain oil and gas fields and other areas having petroleum potential.

Miscellaneous Field Studies Maps are multicolor or black-and-white maps on topographic or planimetric bases on quadrangle or irregular areas at various scales. Pre-1971 maps show bedrock geology in relation to specific mining or mineral-deposit problems; post-1971 maps are primarily black-and-white maps on various subjects such as environmental studies or wilderness mineral investigations.

Hydrologic Investigations Atlases are multicolored or black-and-white maps on topographic or planimetric bases presenting a wide range of geohydrologic data of both regular and irregular areas; principal scale is 1:24,000 and regional studies are at 1:250,000 scale or smaller.

Catalogs

Permanent catalogs, as well as some others, giving comprehensive listings of U.S. Geological Survey publications are available under the conditions indicated below from the U.S. Geological Survey, Books and Open-File Reports Section, Federal Center, Box 25425, Denver, CO 80225. (See latest Price and Availability List.)

"Publications of the Geological Survey, 1879- 1961" may be purchased by mail and over the counter in paperback book form and as a set of microfiche.

"Publications of the Geological Survey, 1962- 1970" may be purchased by mail and over the counter in paperback book form and as a set of microfiche.

"Publications of the U.S. Geological Survey, 1971- 1981" may be purchased by mail and over the counter in paperback book form (two volumes, publications listing and index) and as a set of microfiche.

Supplements for 1982, 1983, 1984, 1985, 1986, and for subsequent years since the last permanent catalog may be purchased by mail and over the counter in paperback book form.

State catalogs, "List of U.S. Geological Survey Geologic and Water-Supply Reports and Maps For (State)," may be purchased by mail and over the counter in paperback booklet form only.

"Price and Availability List of U.S. Geological Survey Publications," issued annually, is available free of charge in paperback booklet form only.

Selected copies of a monthly catalog "New Publications of the U.S. Geological Survey" available free of charge by mail or may be obtained over the counter in paperback booklet form only. Those wishing a free subscription to the monthly catalog "New Publications of the U.S. Geological Survey" should write to the U.S. Geological Survey, 582 National Center, Reston, VA 22092.

Note.--Prices of Government publications listed in older catalogs, announcements, and publications may be incorrect. Therefore, the prices charged may differ from the prices in catalogs, announcements, and publications.